ACTA IMEKO
ISSN: 2221-870X
June 2026, Volume 15, Number 2, 1 - 20

Monte Carlo-based uncertainty quantification for conformity assessment and traceable calibration of high-frequency instrumentation

Marija Cundeva – Blajer[1], Gjorgji Dimitrovski [1], Monika Nakova[1], Kiril Demerdziev[1]

[1] *Ss. Cyril and Methodius University in Skopje, Faculty of Electrical Engineering and Information Technologies, st. "Rugjer Boshkovikj" No.18, Skopje, Republic of North Macedonia*

ABSTRACT
Calibrating high-frequency instruments, such as oscilloscopes and frequency counters, presents significant metrological challenges due to complex and hard-to-validate measurement procedures, limited SI traceability for high-frequency signals, and multiple uncertainty sources. This paper presents the development of uncertainty models for traceable oscilloscope calibration, conducted within the Laboratory for Electrical Measurements at Ss. Cyril and Methodius University in Skopje, aligned with Euramet cg-7 guidelines. Using an originally created software at the Ss. Cyril and Methodius University in Skopje—the MonteCalc Uncertainty Toolkit—the study compares the uncertainty evaluation results obtained according to the GUM (Guide to the Expression of Uncertainty in Measurement) methodology and by the application of the stochastic Monte Carlo method embedded in the MonteCalc Uncertainty Toolkit. These data fusion approaches are applied to experimental data from a high-frequency calibration of diverse types of oscilloscopes for validation purposes. The resulting uncertainty outcomes from both approaches are then used to perform a conformity assessment of the calibrated devices, utilizing integrated decision-making rules within the MonteCalc Uncertainty toolkit, complying with the international guideline ILAC-G8.

Section: RESEARCH PAPER

Keywords: oscilloscope calibration; high-frequency electrical instruments; Monte Carlo; measurement uncertainty; conformity assessment; LabVIEW™

Citation: M. Cundeva – Blajer, G. Dimitrovski, M. Nakova, K. Demerdziev, Monte Carlo-based uncertainty quantification for conformity assessment and traceable calibration of high-frequency instrumentation, Acta IMEKO, vol. 15 (2026) no. 2, pp. 1-20. DOI: 10.21014/actaimeko.v15i2.2285

Section Editor: Leonardo Iannucci, Politecnico di Torino, Italy

Received January 12, 2026; **In final form** June 8, 2026; **Published** June 2026

Funding: This work was supported by the Ministry of Education and Science of Republic of North Macedonia, the scientific project: "Integrated Metrology-Communication System for Industry 4.0", Grant Contract No. 15-6171/25, from 7.07.2025

Corresponding author: Marija Cundeva-Blajer, e-mail: mcundeva@feit.ukim.edu.mk

1. INTRODUCTION

Accurate measurements in industries like telecommunications, electronics or materials science, are highly dependent on rigorous calibration of high-frequency instruments [1], [2], and [3]. This encompasses the calibration of measurement devices, such as oscilloscopes, counters, vector network analysers, and other microwave measurement systems.

However, three major challenges are identified in the calibration of instruments for high frequencies:

1) Establishment of an unbroken chain of metrological traceability to the primary SI international standards;
2) Identification of the numerous influential factors and building confidential models for the estimation of the uncertainty budget while calibrating instruments for high frequencies;
3) Validation of newly established measurement procedures and methods in the area of the calibration of instruments for high frequencies.

1.1. Issues in establishing international measurement traceability of calibration results of instruments for high frequencies

High-frequency instrument calibration with established international traceability is one of the most frequent challenges in the area of electrical metrology. Due to this, various scientific efforts have been made to contribute to resolving this issue in different areas of application. The current state of the art in the field of calibration and measurement capabilities with confirmed SI traceability within the international community of the most

relevant national metrology institutes (NMIs) in the field of high frequencies is provided in [1].

In [4] and [5] it is described how to characterize the response of a commercial real-time digital oscilloscope (RTDO) with traceability. The commercial RTDO usually deploys a time interleaving analog-to-digital-conversion (ADC) structure, and as a result, it is difficult to obtain an accurate frequency response for each ADC. Therefore, a method is proposed to avoid the under-sampling issue, achieving a high sampling rate.

The contribution [6] provides an example of measurement services based on electro-optic sampling that can be used to establish a traceable calibration chain between high-speed waveform measurements and the SI, through switching to a full waveform metrology paradigm, obtaining an estimate of the central value and associated uncertainty of the entire waveform as a function of time.

An innovative phase measurement method of sinusoidal signals is presented, and a proof-of-concept implementation is demonstrated in [7]. The method allows measuring the phase at the output of a high-frequency sinewave signal generator, with respect to a phase reference signal.

The international metrology community recognizes a persistent gap in high-frequency traceability. It is evidenced in the Key Comparison Database (KCDB) of the International Bureau of Weights and Measures (BIPM), [8], through the published data of the traceable high-frequency upper limits of National Metrology Institutes' (NMIs) calibration and measurement capabilities (CMCs).

In comparison to the previously mentioned publications [4]–[7], the novelty of this contribution is in the experimental setup for the calibration of various oscilloscopes, which is exploited at the Laboratory for Electrical Measurements (LEM) at the Ss. Cyril and Methodius University in Skopje (UKIM), by using a reference standard, a calibrator with established and proven measurement traceability to the primary standards of the BIPM, as it will be presented in detail in Section 2.

1.2. Problems in identification of the influential factors and building reliable models of uncertainty in calibration of instruments for high frequencies

Another challenge in the calibration of high-frequency measurement devices is the accurate evaluation of the uncertainty of calibration results, which imposes computationally intensive modeling due to the numerous significant and often unknown factors, as emphasized in the EURAMET Guideline cg-7 [9].

Some initial analysis of the various factors contributing to the uncertainty budget evaluation while calibrating high-frequency instruments in the Laboratory for Electrical Measurements at UKIM have been presented in contributions [10], [11], [12], and [13].

In this context, the authors of paper [14] propose estimation methods for the sample-time errors, using multiple quadrature signals. To confirm the estimator, they perform Monte Carlo simulation.

A method for waveform calibration with a covariance-based uncertainty analysis is proposed in [15]. The calibration includes an equivalent-circuit model of a generator that can be used to determine how the generator behaves when it is connected to arbitrary loads. From the calibrated waveform vector and its covariance matrix, pulse parameters and their uncertainties are calculated.

The high frequency calibration of the pulse generator using Fast Fourier Transform (FFT) technique for Electromagnetic Compatibility (EMC) testing in the high-frequency domain is presented in [16]. A delay line is inserted into one path as a trigger signal to allow the sampling head of the digital sampling oscilloscope to capture the signal from the other path. This signal waveform is analyzed using FFT and calculated by Matlab to compare with the standard, and the calibration results are shown with an uncertainty budget.

In [17], traceable swept-sine and electrooptic-sampling-system-based sampling-oscilloscope calibrations are applied to measure the systematic error of the nose-to-nose calibration and compare the results to simulations. The results in the paper show that the errors in the nose-to-nose calibration are small at low frequencies, but significant at high frequencies.

Contribution [18] proposes an optical pulse standard method, as a method of evaluating the uncertainty of the calibrated bandwidth of an oscilloscope, where the influencing factors of measurement uncertainty are analyzed and the calculation formula of standard uncertainty is derived. A transfer algorithm of uncertainty is studied, which enables the composite uncertainty of the calibrated bandwidth to be evaluated.

A frequency-selection algorithm for calibrating the impulse-response (vector frequency response) and time base characteristics of Digital Real-Time Oscilloscopes (DRTO) is given in [19]. The objective of the algorithm is to allow the DRTO to be calibrated as closely as possible to a chosen frequency grid while optimizing oversampling and time base fidelity, as well as minimizing the uncertainty contribution due to instrument impairments.

Paper [20] deals with the uncertainty evaluation of the rise time of one pulse of an electrical fast transient burst (EFT/B), as carried out by the National Institute of Metrology, Quality and Technology (Inmetro) of Brazil. The uncertainty sources considered in this evaluation are: the oscilloscope resolution and calibration of voltage and time scale, in the Y-and X-axes, respectively; the bandwidth of the measurement system; the oscilloscope sampling rate; and the repeatability of ten different measurements. In this research, it is discussed that two components stood out for their huge relative contribution: time reading and repeatability. Based on explicit quantitative data, it is concluded that the combined relative contribution of the oscilloscope interpolation function components is larger than the relative contribution of repeatability.

In this contribution, a data fusion procedure originally developed in LEM is, for the first time, applied for estimating the uncertainty of the calibration results of various quantities measured by different types of oscilloscopes at very high frequencies up to 500 MHz. This presents a novelty in the methodology approach, as well as an extension of the upper frequency limit, when benchmarked against the already published research [10]–[20].

1.3. Challenges in validation of measurement procedures in calibration of instruments for high frequencies

Validating newly developed calibration methods is also difficult due to the scarcity of appropriate metrological facilities, reduced options for proficiency testing schemes, inter-laboratory comparisons, and other crucial quality assurance measures that also ensure the confidentiality of calibration results [10], [11], and [12]. This is also visible from the Key Comparison Database (KCDB) of the International Bureau of Weights and Measures (BIPM) [8] in the area of high frequencies.

The Monte Carlo method, as described in the Guide to the Expression of Uncertainty in Measurement (GUM) Supplement 1 [21], [22], uses random sampling techniques to propagate uncertainties through complex measurement models [23]. It demonstrates visible advantages for high-frequency measurement devices, because of the nonlinear and stochastic nature of this type of measurement. Monte Carlo simulations offer a robust statistical approach to estimating uncertainty in calibration functions by modeling a wide range of possible measurement outcomes. The effectiveness of the Monte Carlo approach is demonstrated in a range of high-frequency metrology applications.

For instance, in [24], the application of the Monte Carlo approach in the calibration of microwave systems shows that it can significantly reduce bias and improve the accuracy of uncertainty estimates. Similarly, in [23], the use of Monte Carlo simulations in evaluating the uncertainty of calibration functions, emphasizes its superiority over traditional methods.

An enhancement of the Physikalisch-Technische Bundesanstalt's (PTB) ultrafast optoelectronic measurement facility by characterizing the full impulse and step response of a 70-GHz sampling oscilloscope is presented in [25], by the implementation of a novel optoelectronic technique for the generation and the detection of ultrashort voltage pulses, which serve as calibration signals for the oscilloscope. The uncertainty of the oscilloscope's time-domain response is derived from a Monte Carlo analysis, which enhanced technique considerably reduces the uncertainty of rise-time measurements.

An error vector magnitude (EVM) measurement method for Wideband Code Division Multiple Access (W-CDMA) source is proposed in [26], using a real time oscilloscope with traceability to SI unit, where the measurement uncertainty is evaluated based on a Monte-Carlo simulation, which takes into account the errors from the oscilloscope and signal processing.

Other contributions, like [27], [28], and [29], validate the adequacy of these methodologies in diverse high-frequency or similar calibration cases studies.

In this paper, a new advanced measurement uncertainty model for oscilloscope calibration designed by the Laboratory for Electrical Measurements (LEM) is presented. To evaluate uncertainty, the MonteCalc Uncertainty Toolkit [2], [30], and [31] is deployed, an original LabVIEW™-based software that integrates traditional GUM methodologies [21], [32] with stochastic Monte Carlo simulations [22]. The study compares these two methods using calibration data from a 3 GHz high-frequency oscilloscope [1], and also from two other oscilloscopes: one with a frequency range up to 100 MHz, and another with a frequency range up to 70 MHz. By leveraging the Monte Carlo uncertainty propagation, the toolkit automatically evaluates the device's conformity against integrated decision-making rules at specific measurement points, which is a novelty in comparison to the previously published research in [10]–[13] and [23]–[29].

2. OSCILLOSCOPES CALIBRATION APPROACH IN THE CASE STUDY LABORATORY FOR ELECTRICAL MEASUREMENTS

The Laboratory for Electrical Measurement has established accreditation for the calibration of electrical quantities instruments in compliance to ISO 17025:2017 since 2015, [33]. The scope of accreditation includes the method for calibration of high-frequency instruments, like oscilloscopes, counters, or function generators [1]. This method is aligned with the Calibration Guide EURAMET cg-7 [9]. As a primary reference standard for calibration of oscilloscopes, a Multifunctional Calibrator with a built-in option for the calibration of high-frequency instruments (oscilloscopes and counters) with a frequency range up to 630 MHz [34] is used in LEM. The high-frequency reference standard in LEM is shown in Figure 1.

Figure 1. High frequency reference standard of the Laboratory for Electrical Measurements.

The high-frequency measurement traceability of the reference standard is ensured through its calibration in the producer's accredited calibration laboratory, further traceable to the NMI of the United Kingdom, the National Physical Laboratory (UK NPL), and the international primary reference standards (BIPM).

The calibration guide for oscilloscopes EURAMET cg-7 anticipates a two-stage calibration: 1) vertical deflection calibration (voltage amplitude measurement along the vertical axis), and 2) frequency bandwidth calibration (frequency measurement along the horizontal axis), which are independent from each other. The LEM calibration procedure, compliant to the calibration guide EURAMET cg-7, foresees each set value, produced by the reference standard, repeatedly to be measured 12 times.

The validity of the developed calibration procedure is confirmed by applying it to a real-case scenario of three oscilloscopes with various frequency bandwidths.

The first artefact of calibration (Unit Under Test No.1 – UUT1) is a 3 GHz 4-channel Oscilloscope [35], presented in the

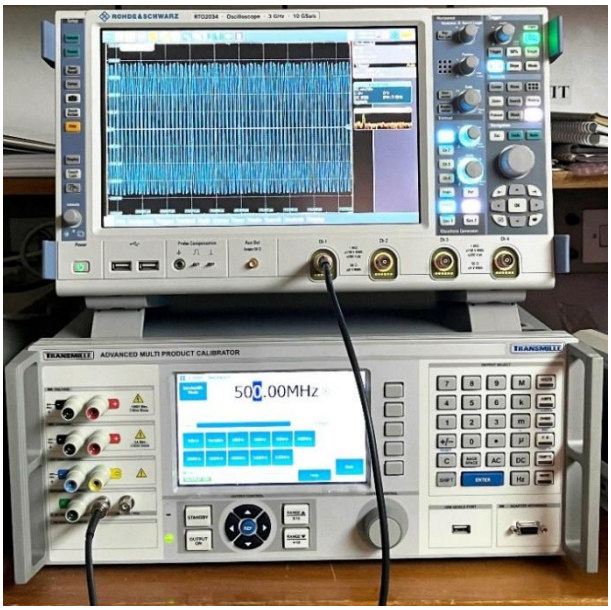

Figure 2. Experimental setup for calibration of UUT1 - 3 GHz 4-channel oscilloscope in the high frequency measurement range.

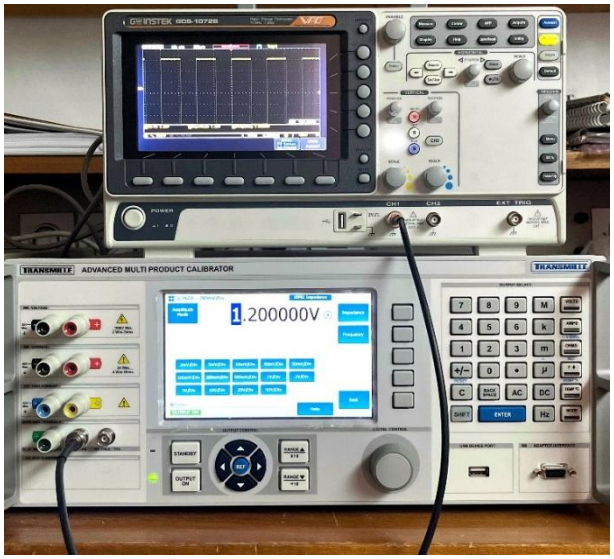

Figure 3. Test setup for calibration of UUT2 - 100 MHz Digital oscilloscope in the voltage amplitude measurement range.

LEM's experimental setup in Figure 2. The UUT1 is a high-accuracy class test equipment for telecommunications with a high-frequency bandwidth.

The second artefact of calibration (Unit Under Test No.2 – UUT2) is a 100 MHz Digital Oscilloscope [36], displayed in the LEM's test setup in Figure 3. The UUT2 is a test equipment predominantly used in the electronics automotive supply chain sector.

The third artefact of calibration (Unit Under Test No.3 – UUT3) is a 70 MHz Digital Oscilloscope, [37], shown in the LEM's laboratory configuration in Figure 4. The UUT3 is a test equipment mostly applied for educational purposes, as well as in fundamental research and development measurement and industrial applications.

An original LEM data fusion concept, presented in [32], is applied to gain the uncertainty budget for the two calibration stages. Namely, data from a component of type A and components of type B are fused, following the guidelines of GUM [21], aligning with the recommendations of the EURAMET guide [9]. Type A uncertainty u_{A}, is obtained through statistical processing of experimental data, by the mean value, X_{mean}, as the measurement's standard deviation, as follows:

$$u_{\mathrm{A}} = \sqrt{\frac{1}{n-1}\sum_{i=1}^{n}(X_{i\,\mathrm{cor}} - X_{\mathrm{mean}})^2}\ , \tag{1}$$

where

$$X_{\mathrm{mean}} = \frac{1}{n}\sum_{i}^{n} X_{i\,\mathrm{cor}}\ , \tag{2}$$

$$X_{i\,\mathrm{cor}} = X_i - X_{\mathrm{ref}}\ . \tag{3}$$

X_i is the measured value in the specific measurement point and X_{ref} is the value generated from the reference standard. The uncertainty inputs of type B, which are fused in the uncertainty budget u_{B} are as follows.

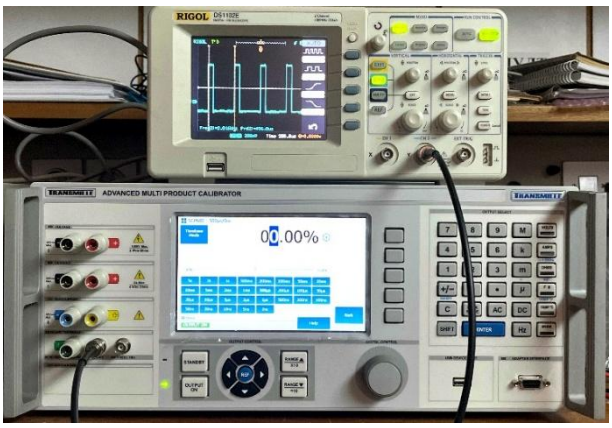

Figure 4. Laboratory configuration for calibration of UUT3 - 70 MHz Digital storage oscilloscope in the bandwidth estimation range.

The input from the resolution of the calibrated instrument, $u_{\mathrm{res\_insrt}}$ is computed as:

$$u_{\mathrm{res\_insrt}} = \frac{resolution\_of\_the\_instrument}{2\cdot\sqrt{3}}\ . \tag{4}$$

The input from the resolution of the reference standard, $u_{\mathrm{res\_insrt}}$ is computed as:

$$u_{\mathrm{res\_refst}} = \frac{resolution\_of\_the\_reference\_standard}{2\cdot\sqrt{3}}\ . \tag{5}$$

In equations (4) and (5), the uncertainty components are calculated by assuming a uniform distribution, where half resolution (resolution/2) equals the distribution's half-width and the division by $\sqrt{3}$ is performed to obtain the standard uncertainty from the distribution half-width.

The uncertainty input component corresponding to the accuracy and the drift of the reference standard $u_{\mathrm{d\_refst}}$, is calculated as:

$$u_{\mathrm{d}} = \frac{\frac{U_{\mathrm{d,\%}}}{100}\cdot X_{\mathrm{REF}} + DRIFT}{2}\ . \tag{6}$$

It is calculated as given in the specifications of the calibrator, i.e. the reference standard [34]. It has two components, a percentage accuracy $U_{\mathrm{d,\%}}$ of the sourced value X_{REF} and a fixed drift. In the calibrator's manual, [34] it is presented for a coverage interval of approximately 95 %, assuming Gaussian distribution, hence the division by coverage factor of $k = 2$ for obtaining the standard uncertainty.

The input from the calibration of the reference standard $u_{\mathrm{cal\_refst}}$ is calculated from the data available in its calibration certificate $U_{\mathrm{cal\_rs}}$. As the calibration uncertainty $U_{\mathrm{cal\_rs}}$ is usually comprised of several influencing factors, and it is presented for coverage interval of approximately 95 %, normal distribution and division by factor of $k = 2$ are adopted.

$$u_{\mathrm{cal\_refst}} = \frac{U_{\mathrm{cal\_rs}}}{2}\ . \tag{7}$$

U_{CAL} is the calibration uncertainty in absolute form, the way it is presented in the calibration certificate of the reference standard.

The combined uncertainty of type B stands for:

$$u_{\mathrm{B}} = \sqrt{u^2_{\mathrm{res\_inst}} + u^2_{\mathrm{res\_refst}} + u^2_{\mathrm{d\_refst}} + u^2_{\mathrm{cal\_refst}}}\ , \tag{7}$$

while the total combined uncertainty is:

$$u_c = \sqrt{u_A^2 + u_B^2}\,. \tag{8}$$

The expanded uncertainty, necessary as an input in the decision process for conformity statement, is:

$$U = 2 \cdot u_c\,. \tag{9}$$

It is important to note that the presented methodology for the calculation of the measurement uncertainty is valid both for the uncertainty of the vertical deflection calibration and the horizontal deflection calibration, as well as for the oscilloscope's bandwidth calibration.

The detailed calculation of the particular uncertainty components following the presented data fusion concept, and the discussion of their contribution to the total combined uncertainty of some of the presented results in Section 4, are already published in [1]. However, the same validated methodology is further applied for all the results presented in this contribution.

3. DESCRIPTION OF THE ORIGINALLY DEVELOPED SOFWARE – MONTECALC UNCERTAINTY TOOLKIT

The software which is applied for modelling uncertainty according to the GUM and the Monte Carlo methodology, and further for the conformity assessment of the calibration results was originally developed by LEM in the programming platform of LabVIEW™ [38]. LabVIEW™ is a graphical programming language that allows options on evolving virtual instrumentation from the appearance of the user interface to the program structure. The developed virtual instrument complies to a satisfactory degree with the following recommendable features:

- scalability: a measure of how easily a program can be extended to perform more tasks;
- maintainability: adding new features to a program without reprogramming; and
- readability: a measure of how easy it is to review a program and understand its function.

By using LabVIEW, modular programs are created, i.e. the problem is separated into smaller modules conducting specific functions. While programming, special attention is given to the coupling of the modules and to the cohesion—the measure of how well a module performs its function. The virtual instruments should have a low coupling and a high cohesion of modules. So, a module should be so good at performing one function that it does not need to perform anything else.

The originally developed program MonteCalc Uncertainty Toolkit is packaged in a folder with appropriate drivers and is in a format of an .exe file, which allows it to be used without installing the entire LabVIEW™ package. When the .exe file is launched, the Set-Up window shown in Figure 5 opens. The Set-Up window has the functionalities to enter the following input data: a calibration name, Type B components, measurement results. The number of measurements and Type B components that can be entered is practically unlimited. The start of the calculation and the ending of the program also happen through the Set-Up window.

By pressing the Calculate button, two new virtual instruments are automatically created, and the measurement uncertainty budget is calculated according to the two options: the GUM methodology and the Monte Carlo simulation. The newly created virtual instruments are denoted as GUM _ Calibration name from Set UP and MonteCarlo _ Calibration name from Set Up. The names of the new instruments are added to the List control. The virtual instrument for calculating the measurement uncertainty budget, based on the GUM has the following functionalities:

- automatic calculation of the measurement uncertainty budget based on the parameters entered in Set-Up;
- automatic calculation of the compliance graphs depending on a limit value that is set with appropriate control;
- saving results in .jpeg for the compliance graphs and saving the budget in .csv format;
- automatic scaling of the y and x axes of the compliance graphs in order to obtain greater visibility of the results;
- selection of the number of random variables, and distribution partitions;
- automatic calculation of fit graphs depending on a threshold value that is set with appropriate control;
- saving the final distribution and fit graphs in .jpeg format, and the simulation results in .csv; and
- automatic scaling of the y and x axes of fit graphs to obtain greater visibility of results.

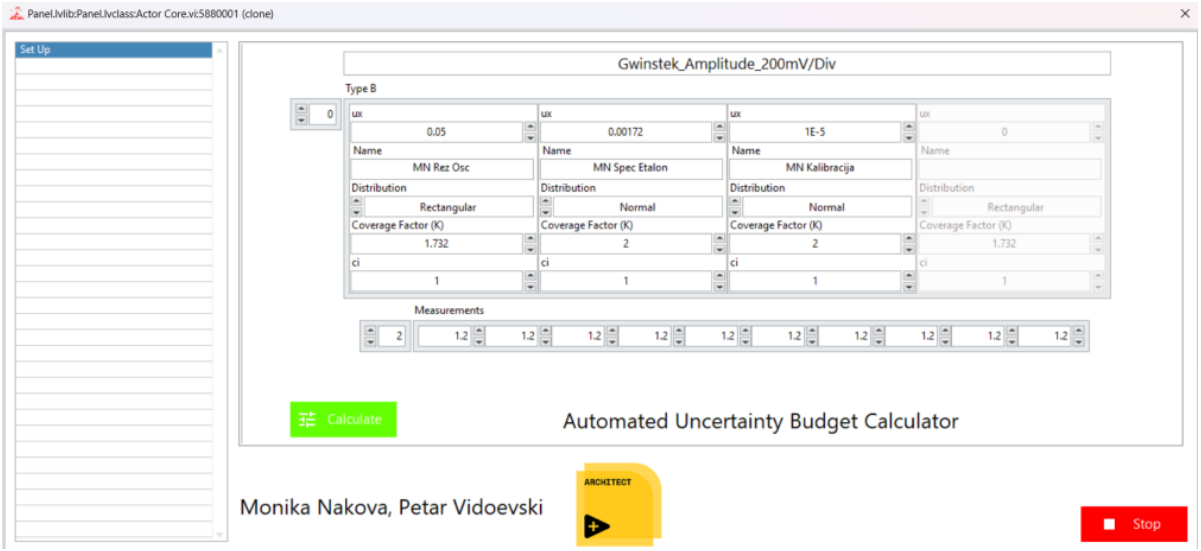

Figure 5. Set-Up window of MonteCalc Uncertainty Toolkit.

The Monte Carlo simulation is conducted by applying a virtual instrument palette enabling the generation of random numbers with an appropriate distribution. The generation of the distribution is done related to the input type B parameters. For each type B component, a distribution of random numbers is generated and summed together with the type A component. The uncertainty for the Monte Carlo simulation is calculated, based on the summed distribution.

Each Monte Carlo simulation generates a random variable depending on the distribution of the input variable. According to Supplement 1 to the "Guide to the expression of uncertainty in measurement — Propagation of distributions using a Monte Carlo method" [22], a value of M, the number of the Monte Carlo trials, i.e. the number of model evaluations to be made, needs to be selected. It can be chosen a priori, in which case there will be no direct control over the quality of the numerical results provided by the Monte Carlo method. The reason is that the number of trials needed to provide these results to a prescribed numerical tolerance will depend on the "shape" of the probability distribution function (PDF) for the output quantity and on the coverage probability required. Also, the calculations are stochastic in nature, being based on random sampling. According to [22], the choice of a value of M that is large compared with $1 / (1-p)$, e.g. M at least 10^4 times greater than $1 / (1-p)$, where p is the required probability, should be made. So, the number of necessary simulations to be performed is determined as in equation (11):

$$M > \frac{10^4}{1-p}. \tag{10}$$

For a probability of 95 %, $p = 0.95$, the number of simulations is equal to 200,000. In most cases, when using Monte Carlo, as in this research, 10^6 simulations are used. According to [22], a value of $M = 10^6$ can often be expected to deliver a 95 % coverage interval for the output quantity such that this length is correct to one or two significant decimal digits. The higher the number of simulations, the better the result. However, an optimisation needs to be conducted between the number of simulations, and the engaged processing power.

As Supplement 1 to the GUM [22] states there is no guarantee that any specific pre-assigned number will suffice, it allows a procedure that selects M adaptively, i.e. as the trials progress. Therefore, the MonteCalc Uncertainty Toolkit, based on LabView virtual instrument has been tested on the processing efficiency and quality of the results, under different conditions, i.e. various number of simulations above the minimally required 200,000 as computed according to equation (11). Generally, the toolkit has derived satisfactorily results within reasonable time frames at a high number of simulations, i.e. above 10^6 simulations. However, it has been empirically concluded that in the case studies presented in the paper, the changes of the obtained results are not visible above 10^6 simulations, i.e. the results are converged after 10^6 simulations. Therefore, $M = 10^6$ has been selected as an optimal number of simulations for the case studies of this contribution.

The MonteCalc Uncertainty Toolkit encompasses a complex evaluation module for conformity assessment against different prescribed decision-making rules according to the international Guideline ILAC G8:09/2019 [40]. The embedded decision-making rules in MonteCalc are the binary rule, the binary rule with guard band, the non-binary rule with guard band and with measurement uncertainty, and others.

4. APPLICATION OF THE MONTECALC UNCERTAINTY TOOLKIT FOR UNCERTAINTY ESTIMATION IN CALIBRATION OF OSCILLOSCOPES

The MonteCalc Uncertainty Toolkit has no restrictions on the type of instrument, the physical quantity measured, the range, the type of the probability distribution etc., as it is universal for deployment in any case of testing/calibration uncertainty estimation. So, it is applied for the analysis of the calibration results uncertainty budget of the three artefacts of calibration listed in Section II, for different specific measurement points in the oscilloscopes' two-stage calibration procedures. The two analysis approaches, the traditional GUM and the stochastic Monte Carlo, are conducted. The results presented in this contribution are only selected specific calibration points from the overall calibration protocol of each of the three Units Under Test (UUTs). For enabling further comparative analysis of the results, the same measurement points in calibration of the vertical deflection and in calibration of the horizontal deflection of the three UUTs are selected. Also, for the purpose of a deeper high frequency analysis of the obtained results, a specific high-frequency bandwidth calibration point of the UUT1, the artefact with the highest upper frequency limit is specifically emphasized. This results selection is provided in the following subsections.

Since the international standard ISO/IEC 17025 was first published, the necessity of conformity statements with specifications or standards has been evidently imposed. However, decision rules to address all statements of conformity across the diverse scope of testing and calibration is not predetermined in the last issue of ISO/IEC 17025:2017 [39]. The international guideline ILAC-G8:09/19 [40] provides some general instructions: a) on the methodology to select appropriate decision rules; and b) on compiling the required elements of a decision rule if no standard rules apply, which is in compliance to the guide JCGM 106:2012 [41].

According to the standard [39], the laboratory shall use the decision rule, considering the accompanying risk level related to the applied rule [41], [42]. There is a risk of delivering a wrong decision because of incorrectly estimated measurement uncertainty, but deployment of guard bands decreases the likelihood of making an inappropriate decision. According to [40], the guard band w is defined as:

$$w = |TL - AL|, \tag{12}$$

with the tolerance/specification limit TL and the acceptance limit AL. In [42], a decision-making algorithm for calibration compliance, considering various guard bands, is proposed.

In compliance with equation (12), the following denotation is used in the legends of Figure 7 to Figure 40 representing the obtained measurement results of different calibration points:

w - guard band
U - expanded uncertainty
$TLMax$ - upper tolerance level
$TLMin$ - lower tolerance level
U_{m} - measured value with the accompanying uncertainty
$ALMax$ - upper acceptance level
$ALMin$ - lower acceptance level.

Figure 6, Figure 11, Figure 16, Figure 21, Figure 26, Figure 31, and Figure 36 represent the probability distribution of the various calibration results obtained by the MonteCalc Uncertainty Toolkit. In these figures, the x-axis (abscissa) presents the range of values that may be attributed to the

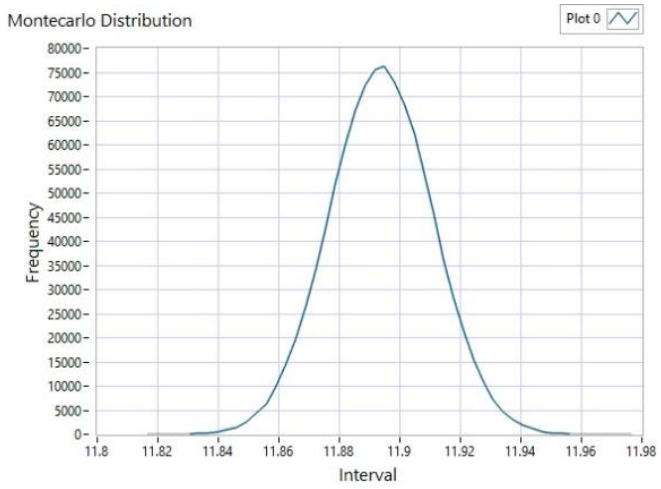

Figure 6. Probability distribution obtained by MonteCalc Uncertainty Toolkit of the vertical deflection calibration at point of 2 V/Div voltage base at Channel 3 of the UUT1.

Table 1. Comparison of the extended measurement uncertainty calculated according to the GUM and Monte Carlo at a calibration point along the vertical axis base of 2 V/Div for the Channel 3 of the UUT1.

Expanded measurement uncertainty GUM U_{GUM}	Expanded measurement uncertainty Monte Carlo simulation U_{MC}	U_{MC} / U_{GUM}
0.02 V	0.05 V	2.5

measured quantity, therefore it is labeled as "Interval", while the y-axis (ordinate) corresponds to the number of repetitive results, regarding the performed Monte Carlo simulation, and hence it is titled "Frequency".

4.1. UUT1 – Selected Results of Vertical Deflection Calibration

For the vertical deflection calibration, the selected point is the 2 V/Div voltage base of the Channel 3 of the UUT1.

Figure 6 displays the probability distribution obtained by the MonteCalc Uncertainty Toolkit, while Table 1 shows the measurement uncertainty results of UUT1 calibration gained from the Toolkit, by applying the GUM approach and by conducting the Monte Carlo simulation, respectively.

From the results in Table 1, it is evident that the expanded measurement uncertainty derived by the Monte Carlo simulation U_{MC} is 2.5 times larger than the expanded uncertainty U_{GUM} estimated by the GUM approach. In this case, the assumption of the normal distribution reduces the uncertainty obtained by the GUM approach.

The derived calibration results of UUT1 with the accompanying uncertainty are subjected to conformity assessment by the built-in option of the MonteCalc Uncertainty Toolkit, against different decision-making rules.

In Figure 7–Figure 10, the compliance graphs obtained by the Monte Carlo simulation method depending on the limit value, set with an appropriate control for the particular decision-making rule, i.e. guard band w, at the calibration point of 2 V/Div voltage base for the Channel 3 of the UUT1, are depicted. The values along the vertical (ordinate) axis in Figure 7–Figure 10 are the measured values of the voltage in Volt V.

Figure 7. Measured result at a calibration point along the vertical axis 2 V/Div voltage base for UUT1 (Channel 3) for w = 0.83 U.

Figure 8. Measured result at a calibration point along the vertical axis 2 V/Div voltage base for UUT1 (Channel 3) for w = U.

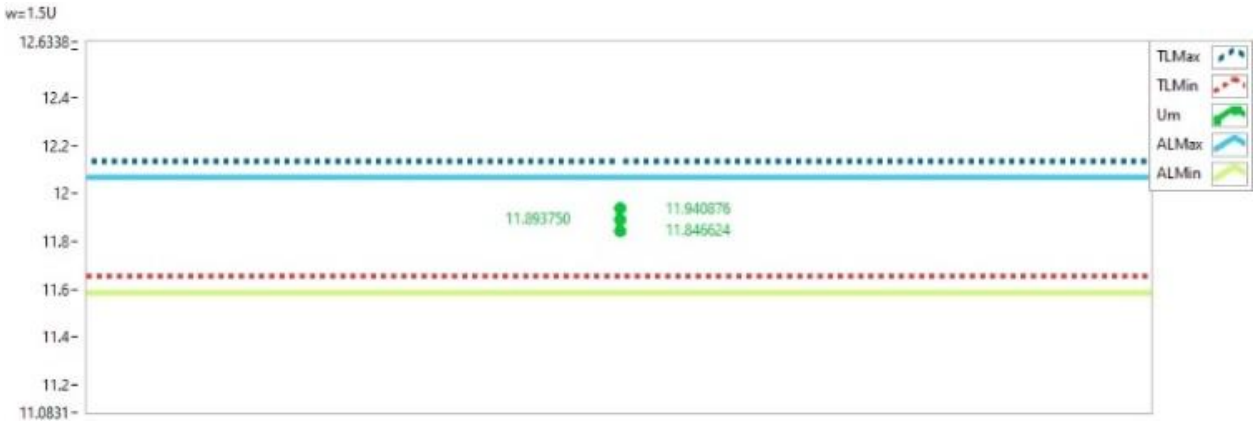

Figure 9. Measured result at a calibration point along the vertical axis 2 V/Div voltage base for UUT1 (Channel 3) for w=1,5U.

Figure 10. Measured result at a calibration point along the vertical axis 2 V/Div voltage base for UUT1 (Channel 3) for w = 3 U.

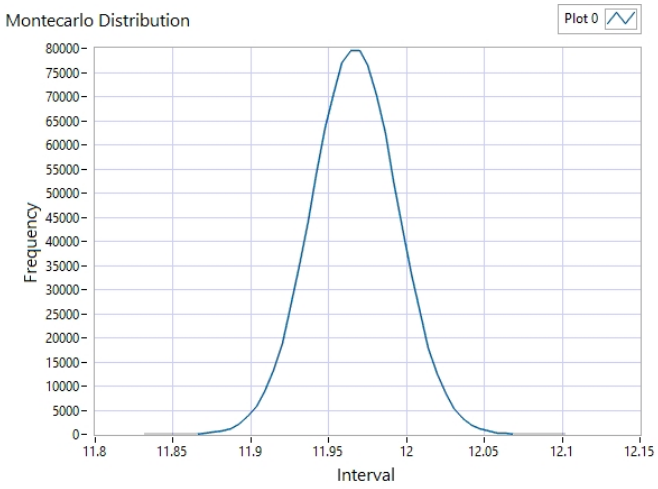

Figure 11. Probability distribution obtained by MonteCalc Uncertainty Toolkit of the vertical deflection calibration at point of 2 V/Div of the UUT2.

Table 2. Comparison of the extended measurement uncertainty calculated according to the GUM and Monte Carlo at a calibration point along the vertical axis of 2 V/Div voltage base of the UUT2.

Expanded measurement uncertainty GUM U_{GUM}	Expanded measurement uncertainty Monte Carlo simulation U_{MC}	U_{MC} / U_{GUM}
0.05 V	0.08 V	1.6

4.2. UUT2 – Selected results of vertical deflection calibration

For the vertical deflection calibration, the selected point is the 2 V/Div voltage base of UUT2. Figure 11 displays the probability distribution obtained by the MonteCalc Uncertainty Toolkit, while in Table 2 are the measurement uncertainty results of UUT2 calibration gained from the Toolkit, by applying the GUM approach and by conducting the Monte Carlo simulation, respectively. The derived calibration results of UUT2 with the accompanying uncertainty are subjected to conformity assessment by the built-in option of the MonteCalc Uncertainty Toolkit, against different decision-making rules.

From the results in Table 2, it is evident that the expanded measurement uncertainty derived by the Monte Carlo simulation U_{MC} is 1.6 times larger than the expanded uncertainty U_{GUM} estimated by the GUM approach.

In this case, the assumption of the normal distribution reduces the uncertainty obtained by the GUM approach. In Figure 12–Figure 15 the compliance graphs obtained by the Monte Carlo simulation method, depending on the limit value set with an appropriate control for the particular decision-making rule, i.e. guard band w, at the calibration point of the 2 V/Div voltage base of the UUT2 are depicted. The values along the vertical (ordinate) axis in Figure 12–Figure 15 are the measured values of the voltage in Volt V.

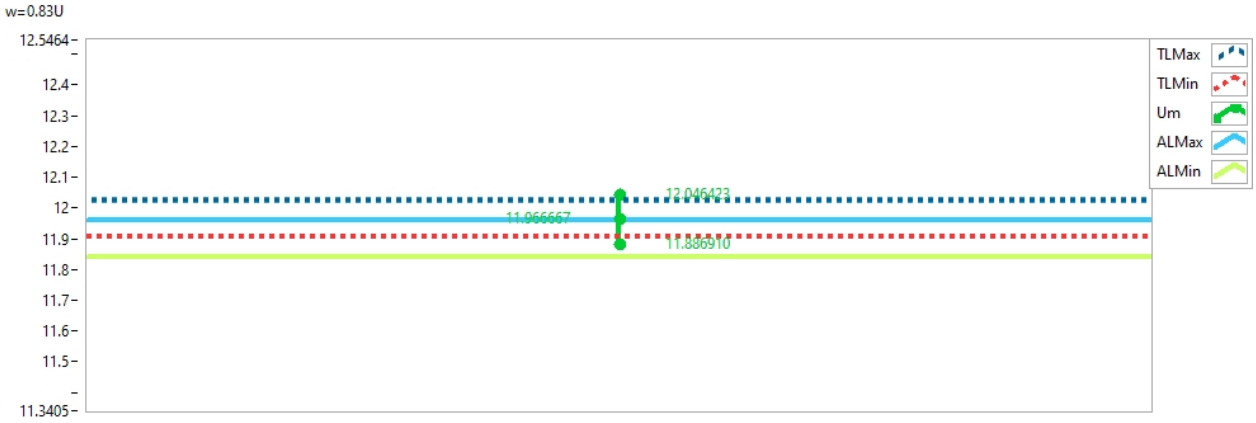

Figure 12. Measured result at a calibration point along the vertical axis 2 V/Div voltage base for UUT2 for w=0,83U.

Figure 13. Measured result at a calibration point along the vertical axis 2 V/Div voltage base for UUT2 for w=U.

Figure 14. Measured result at a calibration point along the vertical axis 2 V/Div voltage base for UUT2 for w=1,5U.

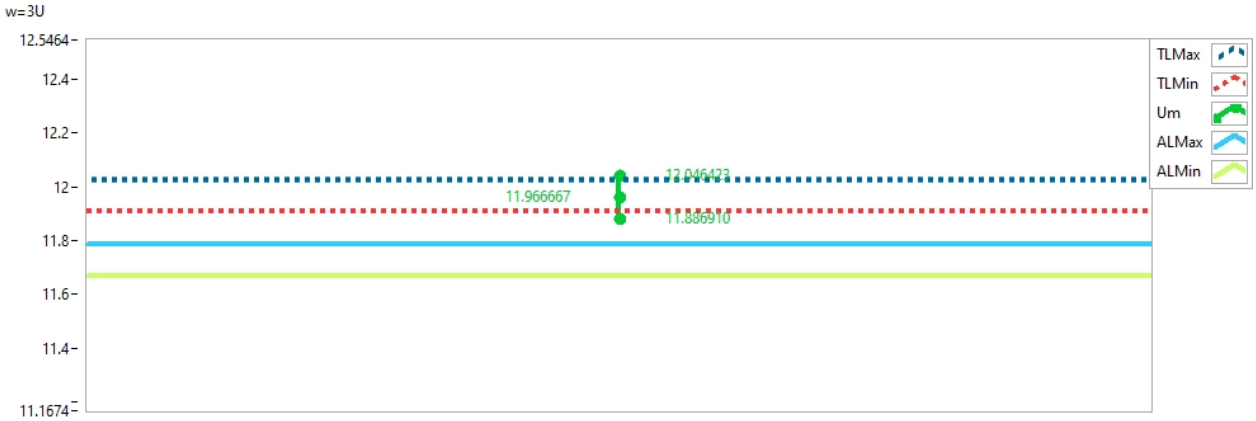

Figure 15. Measured result at a calibration point along the vertical axis 2 V/Div voltage base for UUT2 for w=3U.

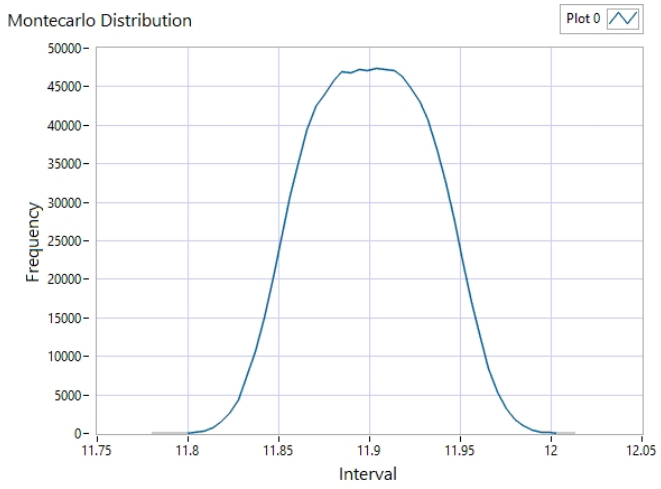

Figure 16. Probability distribution obtained by MonteCalc Uncertainty Toolkit of the vertical deflection calibration at point of 2 V/Div voltage base of the UUT3.

Table 3. Comparison of the extended measurement uncertainty calculated according to the GUM and Monte Carlo at a calibration point along the vertical axis of 2 V/Div voltage base of the UUT3.

Expanded measurement uncertainty GUM U_{GUM}	Expanded measurement uncertainty Monte Carlo simulation U_{MC}	U_{MC} / U_{GUM}
0.06 V	0.069 V	1.2

4.3. UUT3 – Selected results of vertical deflection calibration

For the vertical deflection calibration, the selected point is the 2 V/Div voltage base of the UUT3.

Figure 16 displays the probability distribution obtained by the MonteCalc Uncertainty Toolkit, while Table 3 includes the measurement uncertainty results of the UUT3 calibration, gained from the Toolkit, by applying the GUM approach and by conducting the Monte Carlo simulation, respectively. The derived calibration results of UUT3 with the accompanying uncertainty are subjected to conformity assessment by the built-in option of the MonteCalc Uncertainty Toolkit, against different decision-making rules. From the results in Table 3, it is evident that the expanded measurement uncertainty derived by the Monte Carlo simulation U_{MC} is 1.2 times larger than the expanded uncertainty U_{GUM} estimated by the GUM approach. In this case, the assumption of the normal distribution reduces the uncertainty obtained by the GUM approach.

In Figure 17-Figure 20, the compliance graphs obtained by the Monte Carlo simulation method, depending on the limit value set with an appropriate control for the particular decision-making rule, i.e. guard band w, at the calibration point of the 2 V/Div voltage base of the UUT3 are displayed. The values along the vertical (ordinate) axis in Figure 17-Figure 20 are the measured values of the voltage in Volt V.

4.4. UUT1 – Selected results of horizontal deflection calibration

For the deflection calibration the selected point is the 100 ns/Div time base of the Channel 3 of the UUT1.

In Figure 21 is the probability distribution obtained by MonteCalc Uncertainty Toolkit, while Table 4 shows the measurement uncertainties derived from the Toolkit, by applying

Figure 17. Measured result at a calibration point along the vertical axis 2 V/Div voltage base for UUT3 for w=0,83U.

Figure 18. Measured result at a calibration point along the vertical axis 2 V/Div voltage base for UUT3 for w=U.

Figure 19. Measured result at a calibration point along the vertical axis 2 V/Div voltage base for UUT3 for w=1,5U.

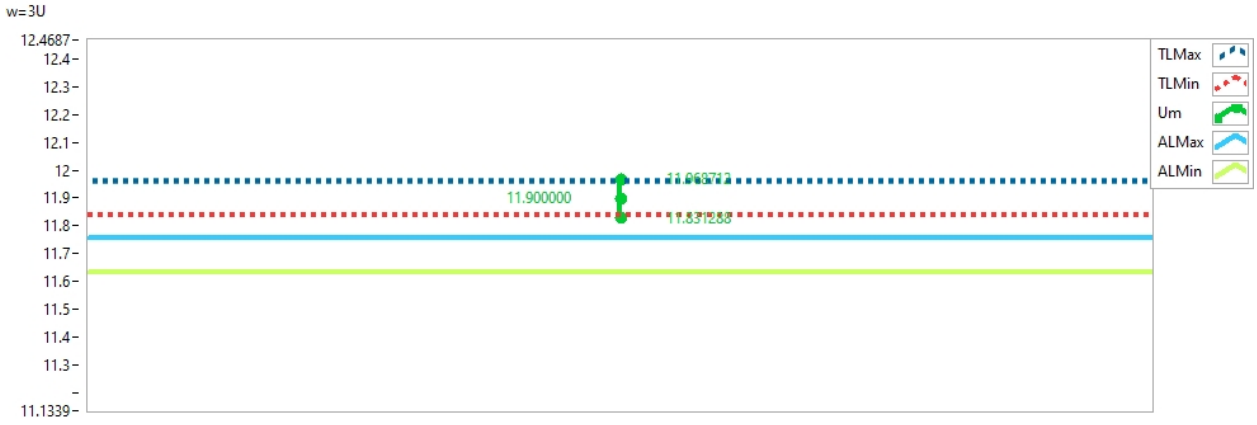

Figure 20. Measured result at a calibration point along the vertical axis 2 V/Div voltage base for UUT3 for w=3U.

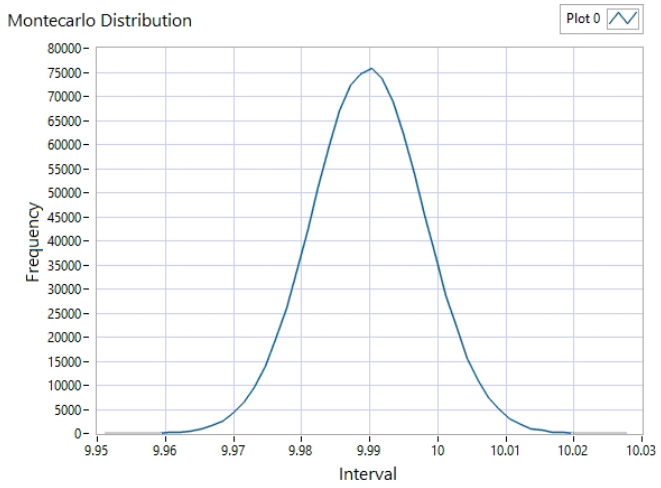

Figure 21. Probability distribution obtained by MonteCalc Uncertainty Toolkit of horizontal deflection calibration at 100 ns/Div time base of the Channel 3 of the UUT1.

Table 4. Comparison of the extended measurement uncertainty calculated according to the GUM and Monte Carlo at a calibration point at 100 ns/Div time base of Channel 3 of the UUT1.

Expanded measurement uncertainty GUM U_{GUM}	Expanded measurement uncertainty Monte Carlo simulation U_{MC}	U_{MC} / U_{GUM}
0.02 MHz	0.02 MHz	1.0

the GUM approach and by the Monte Carlo simulation, respectively. For a better clarity and comparability to the other results in the paper (the bandwidth), the uncertainties in Table 4 are expressed as a reciprocal quantity of the signal time period, i.e. as the frequency uncertainty.

From the results in Table 4, it is evident that the expanded measurement uncertainty derived by the Monte Carlo simulation U_{MC} is the same as the expanded uncertainty U_{GUM} estimated by the GUM approach. In this case, the assumption of the normal distribution applies equally for both approaches.

In Figure 22–Figure 25, the compliance graphs obtained by the Monte Carlo method, depending on the limit value set with an appropriate control for a particular decision-making rule, i.e. guard band w, at the horizontal deflection calibration point of the 100 ns/Div time base of the Channel 3 of the UUT1 are displayed. The values along the vertical (ordinate) axis in Figure 22–Figure 25 are the measured values of the time interval (signal period) in microseconds μs.

4.5. UUT2 – Selected results of horizontal deflection calibration

For the deflection calibration the selected point is the 100 ns/Div time base of the UUT2.

Figure 26 shows the probability distribution obtained by the MonteCalc Uncertainty Toolkit, while, in Table 5, the measurement uncertainties derived from the Toolkit are given, by applying the GUM approach and by the Monte Carlo simulation, respectively. For a better clarity and comparability to the other results in the paper (the bandwidth), the uncertainties in Table 5 are expressed as a reciprocal quantity of the signal time period, i.e. as the frequency uncertainty.

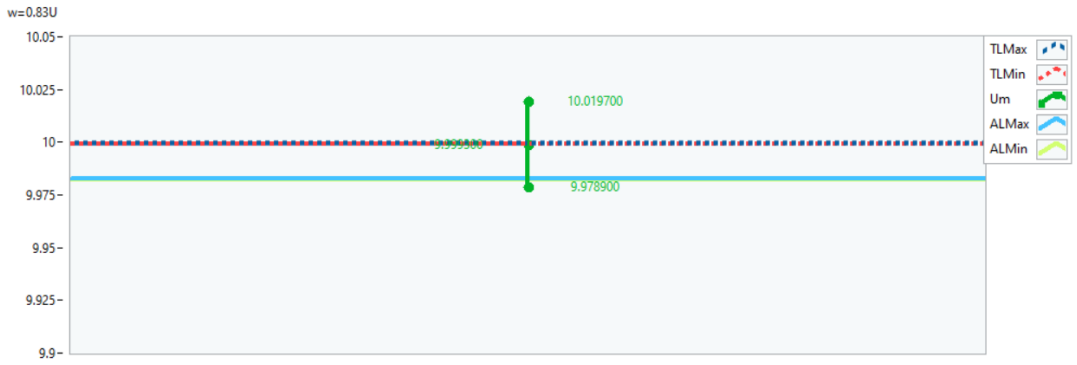

Figure 22. Result at a calibration point of horizontal deflection calibration at 100 ns/Div time base of the Channel 3 of the UUT1 for w=0,83U.

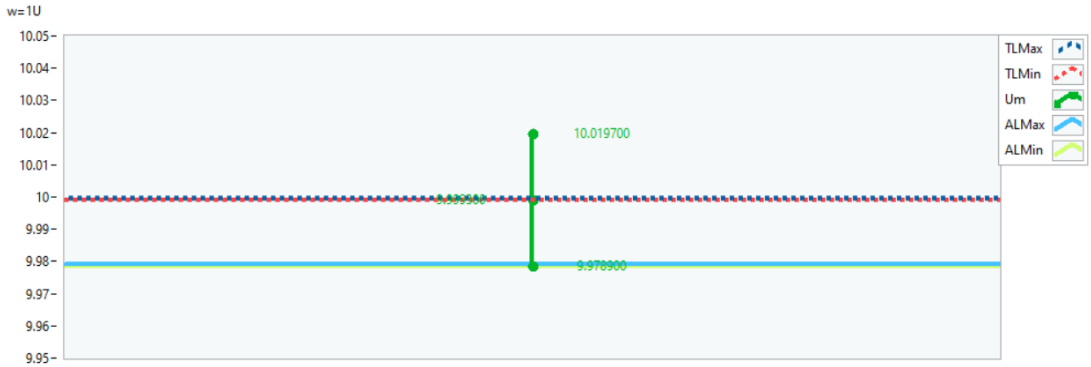

Figure 23. Result at a calibration point of horizontal deflection calibration at 100 ns/Div time base of the Channel 3 of the UUT1 for w=1,0U.

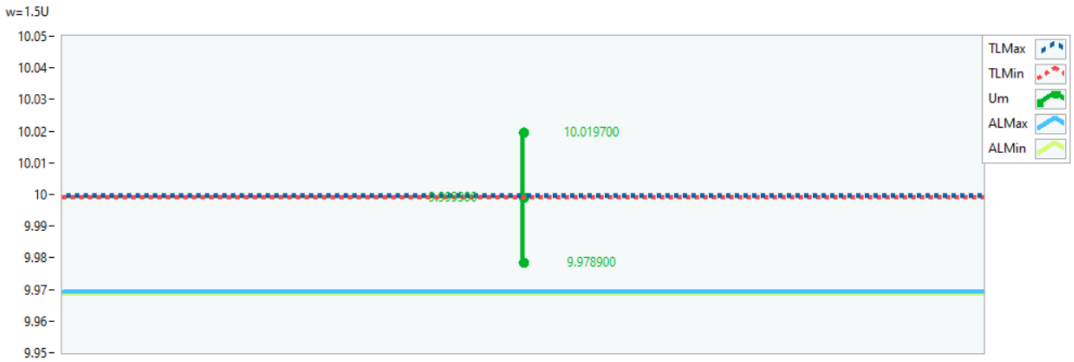

Figure 24. Result at a calibration point of horizontal deflection calibration at 100 ns/Div time base of the Channel 3 of the UUT1 for w=1,5U.

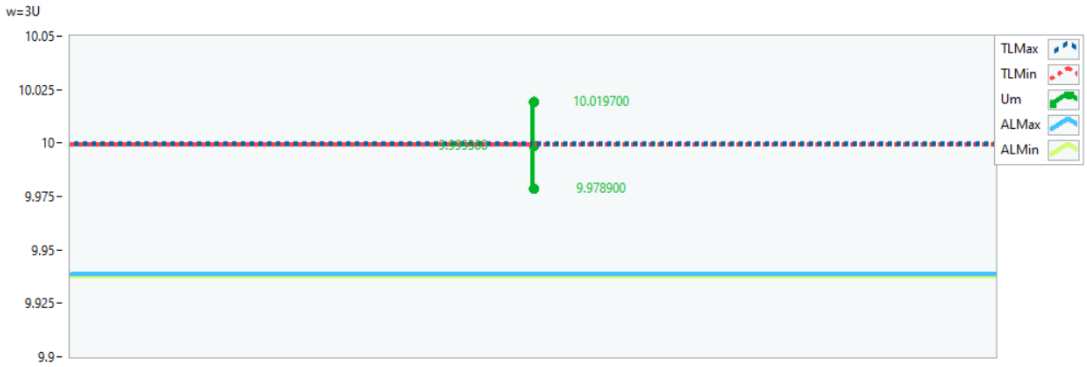

Figure 25. Result at a calibration point of horizontal deflection calibration at 100 ns/Div time base of the Channel 3 of the UUT1 for w=3U.

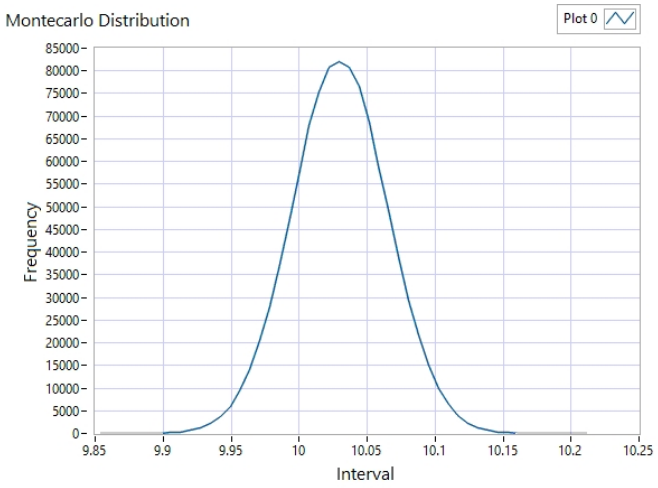

Figure 26. Probability distribution obtained by MonteCalc Uncertainty Toolkit of horizontal deflection calibration at 100 ns/Div time base of the UUT2.

Table 5. Comparison of the extended measurement uncertainty calculated according to the GUM and Monte Carlo at a calibration point at 100 ns/Div time base of the UUT2.

Expanded measurement uncertainty GUM U_{GUM}	Expanded measurement uncertainty Monte Carlo simulation U_{MC}	U_{MC} / U_{GUM}
0.07 MHz	0.11 MHz	1.6

From the results in Table 5, it is evident that the expanded measurement uncertainty U_{MC} derived by the Monte Carlo simulation is 1.6 times larger than the expanded uncertainty U_{GUM} estimated by the GUM approach. In this case, the assumption of the normal distribution reduces the uncertainty obtained by the GUM approach.

In Figure 27–Figure 30, the compliance graphs obtained by the Monte Carlo simulation method, depending on the limit value set with an appropriate control for the particular decision-making rule, i.e. guard band w, at the horizontal deflection calibration point of the 100 ns/Div time base of the UUT2 are displayed. The values along the vertical (ordinate) axis in Figure 27–Figure 30 are the measured values of the time interval (signal period) in μs.

4.6. UUT3 – Selected results of horizontal deflection calibration

For the horizontal deflection calibration, the selected point is the 100 ns/Div time base of the UUT3.

Figure 31 shows the probability distribution obtained by the MonteCalc Uncertainty Toolkit, while, in Table 6, the measurement uncertainties derived from the Toolkit are given, by applying the GUM approach and by the Monte Carlo simulation, respectively. For a better clarity and comparability to the other results in the paper (the bandwidth), the uncertainties in Table 6 are expressed as a reciprocal quantity of the signal time period, i.e. as the frequency uncertainty.

From the results in Table 6, it is evident that the expanded measurement uncertainty derived by the Monte Carlo simulation U_{MC} is twice as large as the expanded uncertainty U_{GUM} estimated by the GUM approach. In this case, the assumption of

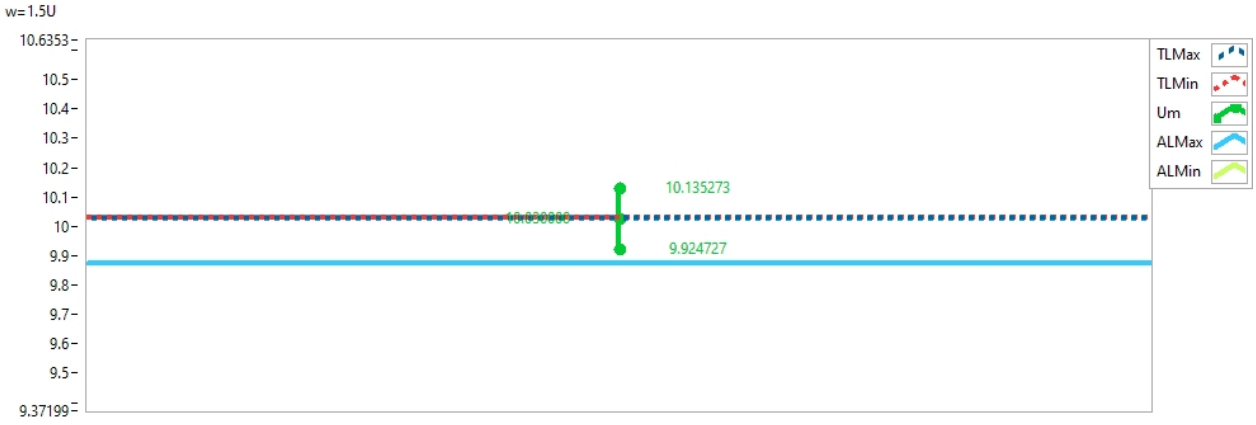

Figure 27. Result at a calibration point of horizontal deflection calibration at 100 ns/Div time base of the UUT2 for w=1,5U.

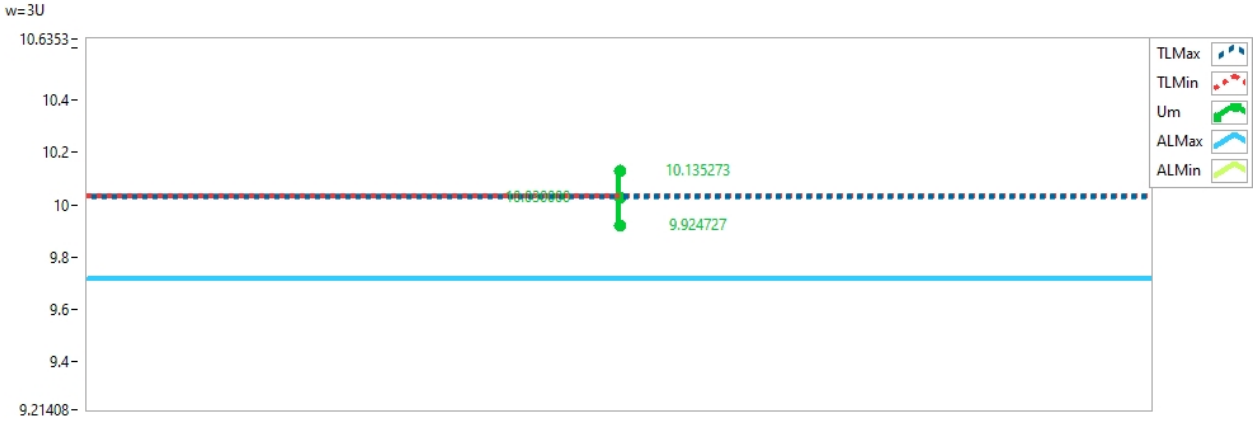

Figure 28. Result at a calibration point of horizontal deflection calibration at 100 ns/Div time base of the UUT2 for w=3U.

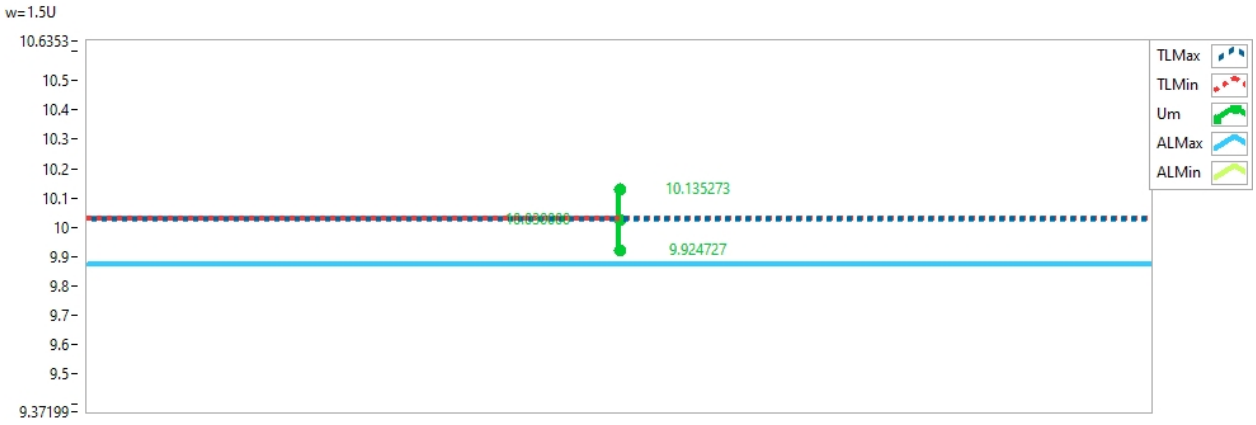

Figure 29. Result at a calibration point of horizontal deflection calibration at 100 ns/Div time base of the UUT2 for w=1,5U.

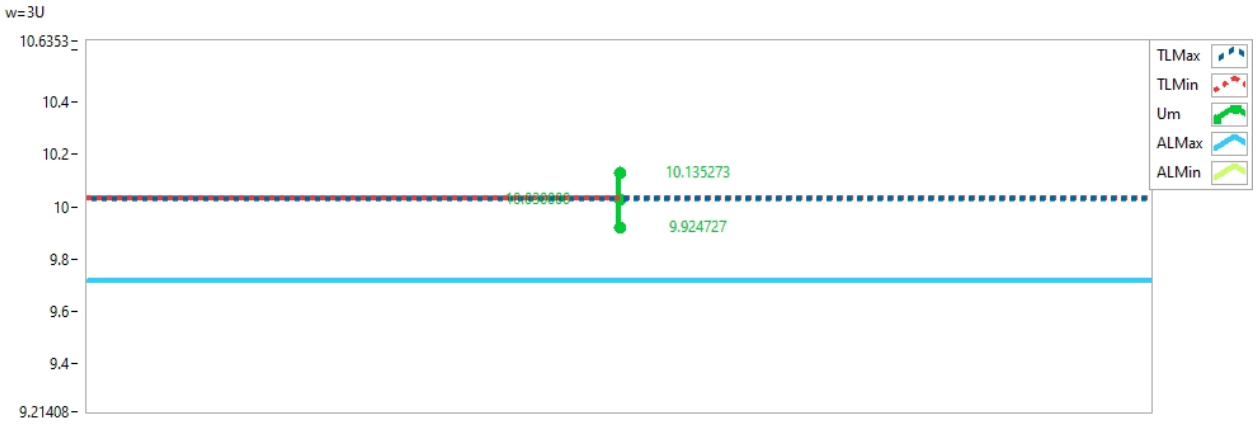

Figure 30. Result at a calibration point of horizontal deflection calibration at 100 ns/Div time base of the UUT2 for w=3U.

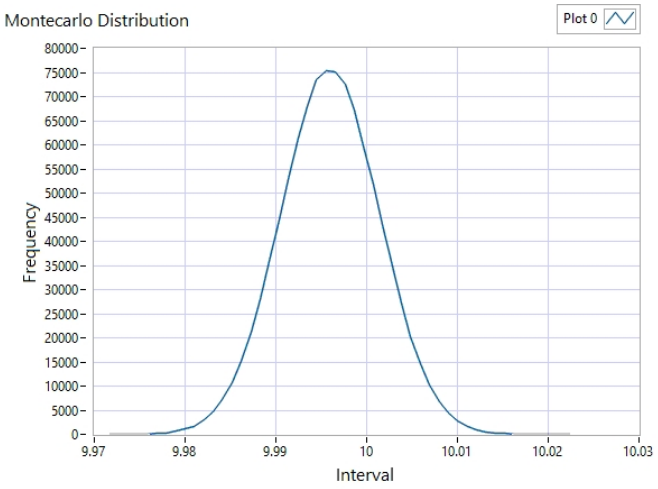

Figure 31. Probability distribution obtained by MonteCalc Uncertainty Toolkit of horizontal deflection calibration at 100 ns/Div time base of the UUT3.

Table 6. Comparison of the extended measurement uncertainty calculated according to the GUM and Monte Carlo at a calibration point at 100 ns/Div time base of the UUT3.

Expanded measurement uncertainty GUM U_{GUM}	Expanded measurement uncertainty Monte Carlo simulation U_{MC}	U_{MC} / U_{GUM}
0.01 MHz	0.02 MHz	2.0

the normal distribution reduces the uncertainty obtained by the GUM approach.

In Figure 32–Figure 35, the compliance graphs obtained by the Monte Carlo simulation method, depending on the limit value set with an appropriate control for the particular decision-making rule, i.e. guard band w, at the horizontal deflection calibration point of the 100 ns/Div time base of the UUT3 are displayed. The values along the vertical (ordinate) axis in Figure 32–Figure 35 are the measured values of the time interval (signal period) in microseconds μs.

4.7. UUT1 – Selected results of high-frequency bandwidth calibration

For the high-frequency bandwidth calibration, the selected point is the 500 MHz for the Channel 2 of the UUT1.
Figure 36 shows the probability distribution obtained by the MonteCalc Uncertainty Toolkit, while, in Table 7, the measurement uncertainties derived from the Toolkit are given, by applying the GUM approach and by the Monte Carlo simulation, respectively. From the results in Table 7, it is evident that the expanded measurement uncertainty U_{MC} derived by the Monte Carlo simulation is 1.7 times larger than the expanded uncertainty U_{GUM} estimated by the GUM approach. In this case, the assumption of the normal distribution reduces the uncertainty obtained by the GUM approach.

In Figure 37–Figure 40, the compliance graphs obtained by the Monte Carlo method, depending on the limit value set with an appropriate control for a particular decision-making rule, i.e. guard band w, at the calibration point of 500 MHz of the UUT1 (Channel 2), are displayed. The values along the vertical

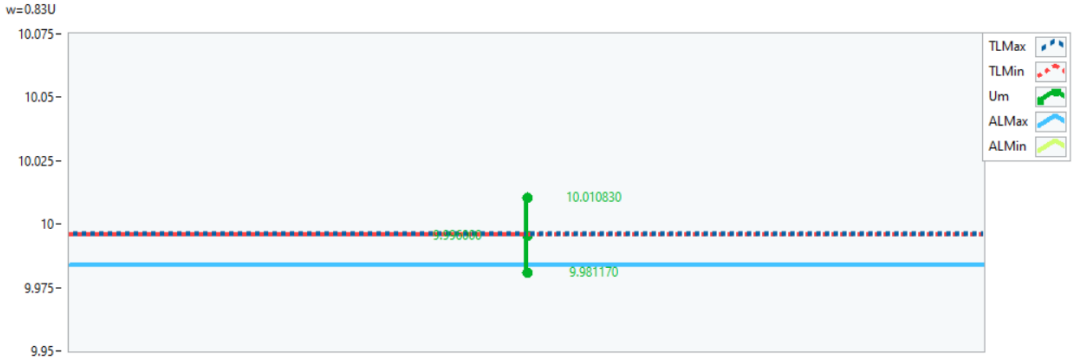

Figure 32. Result at a calibration point of horizontal deflection calibration at 100 ns/Div time base of the UUT3 for w=0,83U.

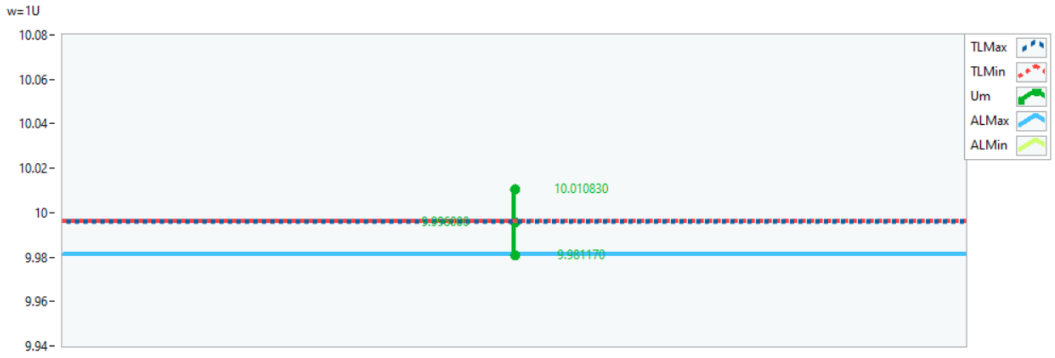

Figure 33. Result at a calibration point of horizontal deflection calibration at 100 ns/Div time base of the UUT3 for w=1,0U.

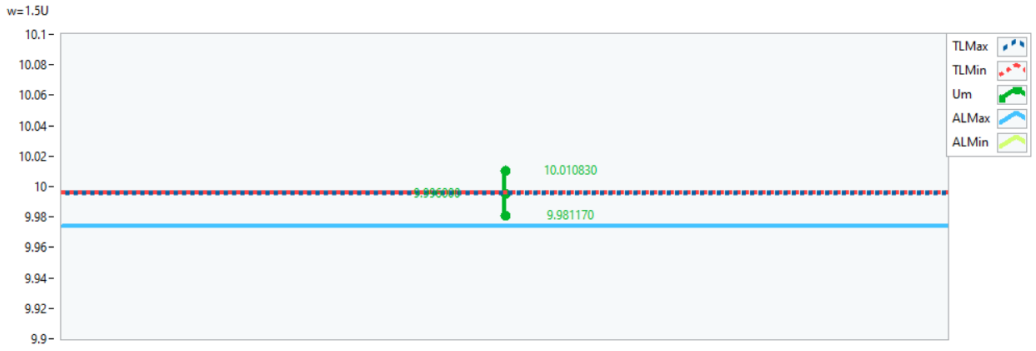

Figure 34. Result at a calibration point of horizontal deflection calibration at 100 ns/Div time base of the UUT3 for w=1,5U.

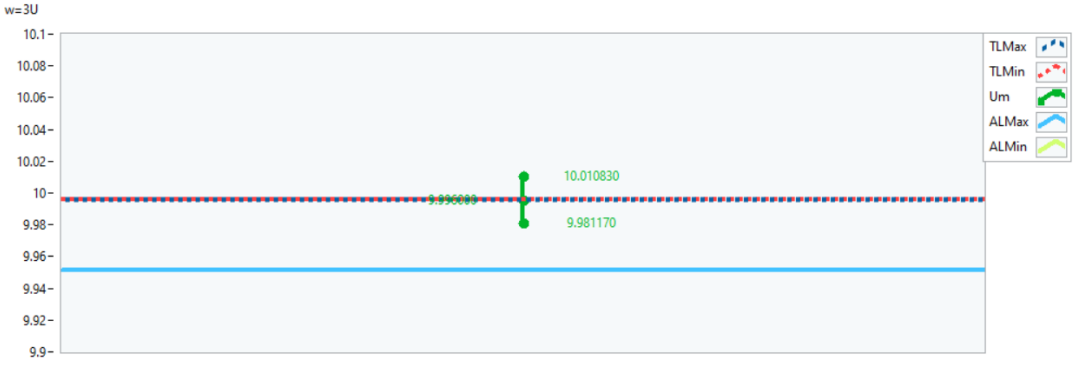

Figure 35. Result at a calibration point of horizontal deflection calibration at 100 ns/Div time base of the UUT3 for w=3U.

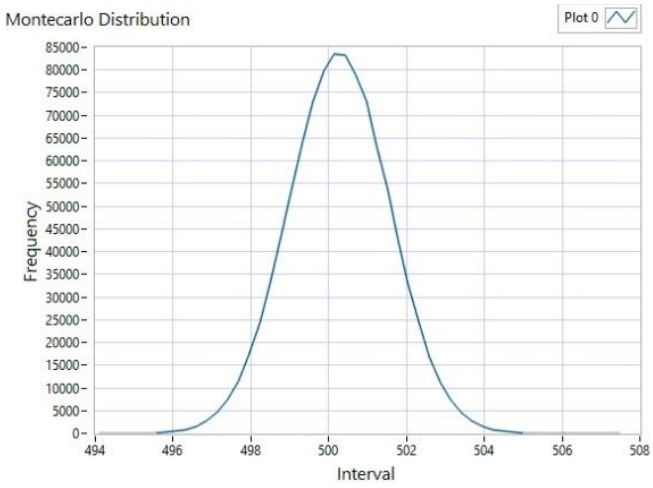

Figure 36. Probability distribution obtained by MonteCalc Uncertainty Toolkit of the frequency bandwidth of 500 MHz Channel 2 of the UUT1.

Table 7. Comparison of the extended measurement uncertainty calculated according to the GUM and Monte Carlo at a calibration point at the frequency bandwidth of 500 MHz Channel 2 of the UUT1.

Expanded measurement uncertainty GUM U_{GUM}	**Expanded measurement uncertainty Monte Carlo simulation U_{MC}**	**U_{MC} / U_{GUM}**
2.3 MHz	3.9 MHz	1.7

(ordinate) axis in Figure 37–Figure 40 are the measured values of the frequency in MHz.

5. DISCUSSION OF THE RESULTS

As presented in Table 1 to Table 7 in Section 4, the Monte Carlo approach in all of the analyzed cases provides equal or higher expanded uncertainty in comparison to the uncertainty evaluated by the GUM approach. In some cases, the uncertainty derived by the Monte Carlo method is twice as large as the GUM-obtained results. It can be concluded that the presumption of the normal distribution evidently affects the outcomes of the uncertainty estimation, i.e. in most of the analyzed cases it reduces the uncertainty of the calibration result, as in the GUM approach.

Based on Figure 6, Figure 11, Figure 16, Figure 21, Figure 26, Figure 31, Figure 36 a qualitative analysis of the skewness (measuring asymmetry) γ_1 and the kurtosis (measuring tailedness) γ_2 of the probability distribution derived by the Monte Carlo simulation can be conducted and certain conclusions can be derived.

Concerning the skewness, dominantly, a high level of symmetry can be observed; however, when closely examined, except in Figure 21, the skewness indicator in most of the cases is positive, $\gamma_1 > 0$, i.e. the right tail is longer, and the mean is greater than the median. In these cases, the ratio of the expanded uncertainty calculated by the Monte Carlo simulation and the expanded uncertainty calculated by the GUM is greater than 1, i.e. $U_{\mathrm{MC}}/U_{\mathrm{GUM}} > 1$. Furthermore, it is obvious that higher γ_1 results in greater ratio $U_{\mathrm{MC}}/U_{\mathrm{GUM}}$. In Figure 21, the skewness indicator is $\gamma_1 = 0$ and the ratio $U_{\mathrm{MC}}/U_{\mathrm{GUM}} = 1$, which confirms the previous conclusion.

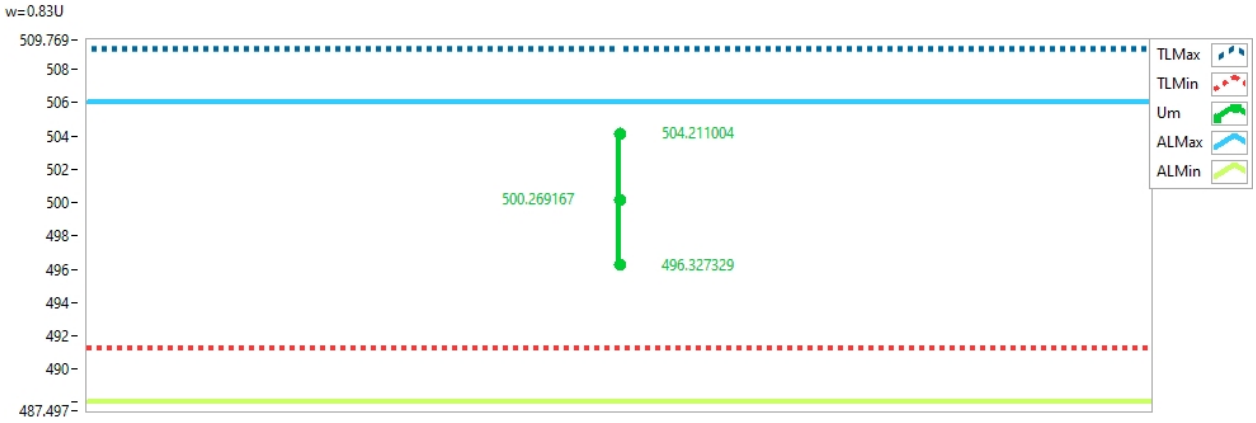

Figure 37. Result at a calibration point of the frequency bandwidth of 500 MHz of the UUT1 (Channel 2) for w=0,83U.

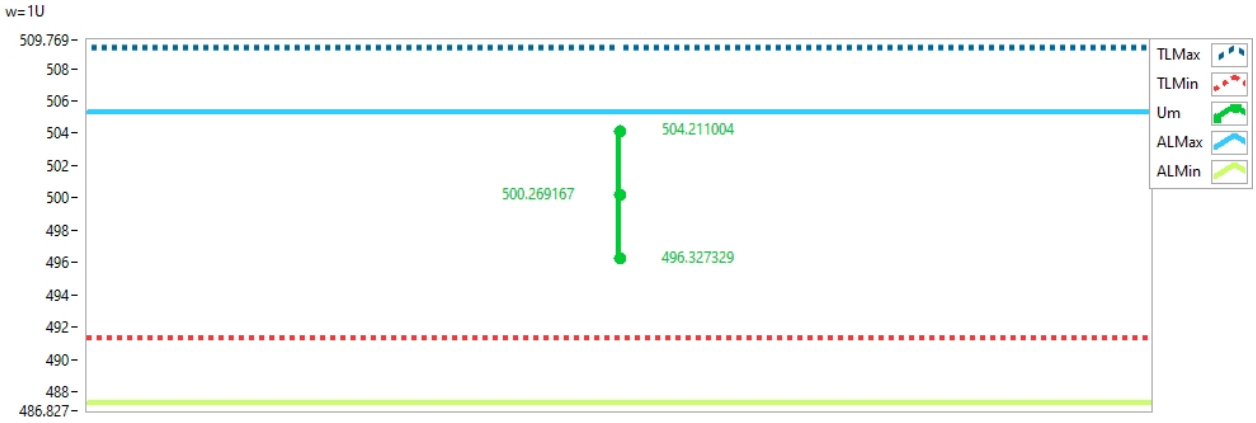

Figure 38. Result at a calibration point of the frequency bandwidth of 500 MHz of the UUT1 (Channel 2) for w=1,0U.

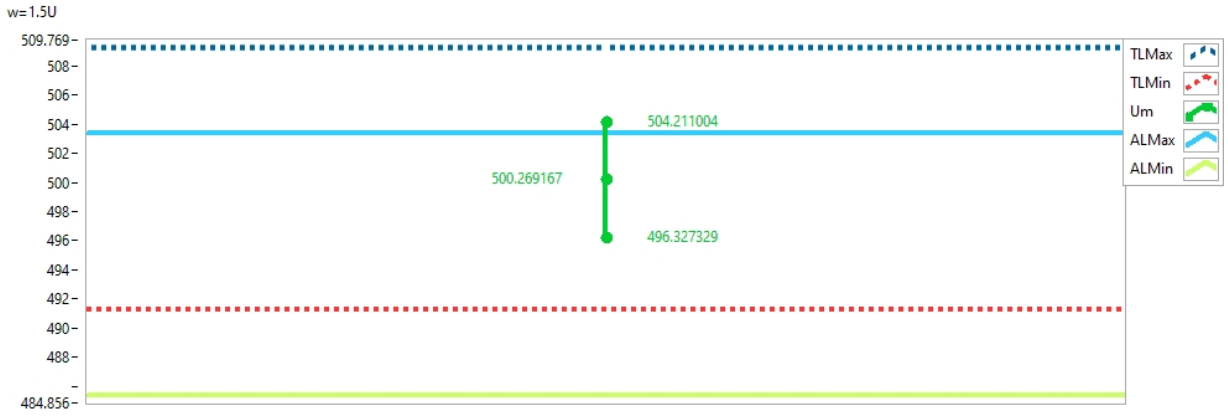

Figure 39. Result at a calibration point of the frequency bandwidth of 500 MHz of the UUT1 (Channel 2) for w=1,5U.

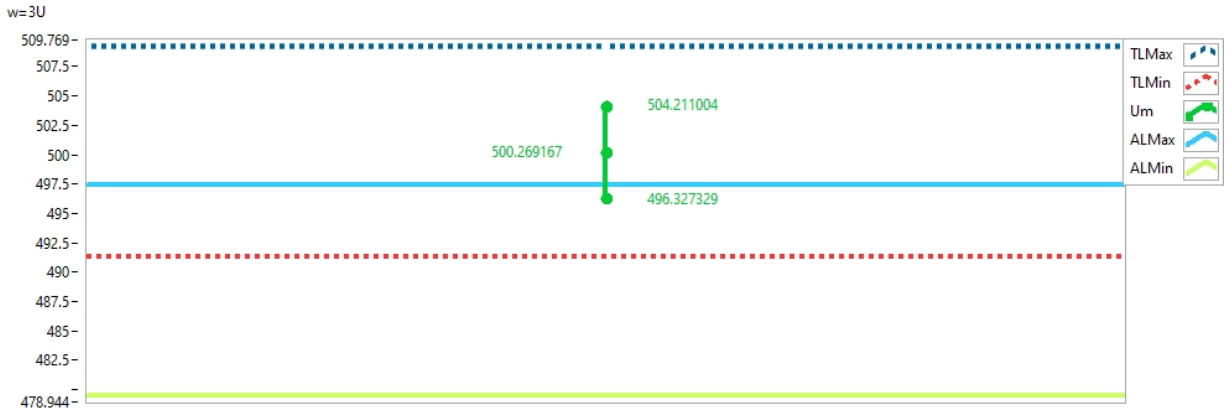

Figure 40. Result at a calibration point of the frequency bandwidth of 500 MHz of the UUT1 (Channel 2) for w=3U.

From the aspect of kurtosis, the only leptokurtic, i.e. "fat" distribution is the one presented in Figure 16, while in the other cases the distributions are tending towards platykurtic "thin" form. However, from the derived quantitative results, a visible relationship between the distribution kurtosis and the ratio of the expanded uncertainty, calculated by the Monte Carlo simulation, and the expanded uncertainty, calculated by the GUM, is complex to be established. Deeper quantitative analysis of the distributions' kurtoses must be conducted to provide a functional relation between the kurtosis indicator and the $U_{\mathrm{MC}}/U_{\mathrm{GUM}}$ ratio.

As the expanded uncertainty is a direct input in the decision-making process related to the compliance of the results, both in the guard band and in the presentation of the measurement results themselves, when compared, the reduced uncertainty imposes the risk of accepting non-compliant results due to lower estimated uncertainty. Therefore, a more conservative approach is adopted in the process of the conformity assessment of the calibrated oscilloscopes based on the derived measurement results. Namely, due to the larger values, the measurement uncertainty results derived by the Monte Carlo method are the inputs in the MonteCalc Uncertainty Toolkit embedded algorithm for decision-making for the conformity assessment of the three calibrated oscilloscopes in various measurement points.

For the purposes of the discussion in Table 8–Table 14, the summarized outcomes of the fulfillment of the acceptance criteria are expressed, according to each decision-making rule at the respective measurement points of the two-stage calibrations of the three UUTs.

The tables are grouped according to the type of calibration conducted: vertical deflection calibration, horizontal deflection calibration, and high-frequency bandwidth calibration.

The following legend symbols are used:

- ✓ - accepted;
- ☑ - conditionally accepted;
- ☒ - conditionally rejected;
- ✖ - rejected.

5.1. Vertical deflection calibration

Table 8. Declarations of conformity at a calibration point on the vertical deflection at 2 V/Div voltage base for UUT1 Channel 3 based on the outcomes for different decision-making rules.

Decision rule w	0.83 *U*	*U*	1.5 *U*	3 *U*
Binary	✓	✓	✓	✓
Binary with guard band	✓	✓	✓	✓
Non-binary with guard band	✓	✓	✓	✓
Non-binary with guard band & measurement uncertainty	✓	✓	✓	✓

Table 9. Declarations of conformity at a calibration point on the vertical deflection at 2 V/Div voltage base for UUT2 based on the outcomes for different decision-making rules.

Decision rule w	0.83 *U*	*U*	1.5 *U*	3 *U*
Binary	✓	✓	✓	✓
Binary with guard band	✓	✖	✖	✖
Non-binary with guard band	☑	☒	☒	✖
Non-binary with guard band & measurement uncertainty	✓	✓	✓	✓

Table 10. Declarations of conformity at a calibration point on the vertical deflection at 2 V/Div voltage base for UUT3 based on the outcomes for different decision-making rules.

Decision rule w	0.83 *U*	*U*	1.5 *U*	3 *U*
Binary	✓	✓	✓	✓
Binary with guard band	✓	✓	×	×
Non-binary with guard band	☑	☑	☒	×
Non-binary with guard band & measurement uncertainty	✓	✓	✓	✓

5.2. Horizontal Deflection Calibration

Table 11. Declarations of conformity at a calibration point on the horizontal deflection at 100 ns/Div time base for UUT1 Channel 3 based on the outcomes for different decision-making rules.

Decision rule w	0.83 *U*	*U*	1.5 *U*	3 *U*
Binary	✓	✓	✓	✓
Binary with guard band	×	×	×	×
Non-binary with guard band	☒	☒	×	×
Non-binary with guard band & measurement uncertainty	✓	✓	✓	✓

Table 12. Declarations of conformity at a calibration point on the horizontal deflection at 100 ns/Div time base for UUT2 based on the outcomes for different decision-making rules.

Decision rule w	0.83 *U*	*U*	1.5 *U*	3 *U*
Binary	✓	✓	✓	✓
Binary with guard band	×	×	×	×
Non-binary with guard band	☒	☒	×	×
Non-binary with guard band & measurement uncertainty	✓	✓	✓	✓

Table 13. Declarations of conformity at a calibration point on the horizontal deflection at 100 ns/Div time base for UUT3 based on the outcomes for different decision-making rules.

Decision rule w	0.83 *U*	*U*	1.5 *U*	3 *U*
Binary	✓	✓	✓	✓
Binary with guard band	×	×	✓	✓
Non-binary with guard band	☒	☒	✓	✓
Non-binary with guard band & measurement uncertainty	✓	✓	✓	✓

5.3. Frequency Bandwidth Calibration

Table 14. Declarations of conformity at a calibration point of the frequency bandwidth of 500 MHz of the UUT1 (Channel 2) according to the outcomes for different decision-making rules.

Decision rule w	0.83 *U*	*U*	1.5 *U*	3 *U*
Binary	✓	✓	✓	✓
Binary with guard band	✓	✓	✓	×
Non-binary with guard band	✓	✓	☑	☒
Non-binary with guard band & measurement uncertainty	✓	✓	✓	✓

The two methods yielded noticeably different uncertainty values, which is expected as the GUM assumes a normal distribution, an assumption that is not fully true in the case of the oscilloscope calibrations in the three specific calibration procedures: the vertical deflection, the horizontal deflection, as well as the high frequency bandwidth calibration. On the other hand, the Monte Carlo simulation takes into account the actual distribution by randomly generating variable values. So, the Monte Carlo approach is more appropriate, as it produces a broader uncertainty range, thus supporting more conservative and reliable conformity assessments.

The outcomes from the conformity assessment presented in Table 8–Table 14 provide diverse acceptance decisions for different decision rules with various applied guard band w. Therefore, the laboratory must prescribe an appropriate decision-making procedure depending on various factors but foremost considering the applicability of the artefact of calibration. It is evident from the outcomes presented above that the UUTs with more rigorous technical specifications demonstrate a higher level of fulfilment of the acceptance criteria. It can be recommended that, for instruments intended for critical applications, more rigorous decision-making rules be applied.

6. CONCLUSIONS

Based on the identified challenges in the field of calibration of high-frequency instruments in the introductory section, a thorough analysis of the uncertainty in the calibration of high-frequency instruments-oscilloscopes, by the application of the standard GUM and the Monte Carlo, has been conducted. The original LEM data fusion concept is embedded in both uncertainty evaluation approaches.

The software originally developed by LEM, MonteCalc Uncertainty Toolkit, implementing both the mainstream GUM and the random Monte Carlo method, is applied in the experimental laboratory calibration of high-frequency instruments of diverse technical specifications. The uncertainty results derived are entries for the decision-making process, also a built-in module within the MonteCalc Uncertainty Toolkit. The study provided that the two evaluation methods, the GUM and the stochastic Monte Carlo simulation, produced evidently different uncertainty values, which is expected and thoroughly discussed in the paper. While GUM assumes a normal distribution, this assumption was found to be not fully appropriate for the three specific oscilloscope calibration procedures: vertical deflection, horizontal deflection, and high-frequency bandwidth, as it reduces the values of the measurement uncertainty up to twice of the values derived with the Monte Carlo methodology. Consequently, the Monte Carlo approach is deemed more suitable as it accounts for actual distributions, resulting in a broader and more conservative uncertainty range that supports more reliable conformity assessments.

From the presented qualitative analysis and discussion, it is concluded that in most of the presented cases there is a positive tendency of the skewness indicator of the distribution probability, i.e. the right tail is longer, and the mean is greater than the median. This is reflected in a higher expanded uncertainty calculated by the Monte Carlo simulation than the one derived by the GUM approach. The kurtoses indicators in the analyzed measurement points are mostly of platykurtic type; however, for the establishment of a firmer relationship between the ratio $U_{\mathrm{MC}}/U_{\mathrm{GUM}}$ and the kurtosis indicator, much deeper quantitative analysis must be conducted, which provides a relevant basis for further research. Such analysis will enable more profound and even more argument-based models for proper decision-making criteria in conformity assessment.

The presented methodology is universal and can be applied in laboratories tending to establish validated and traceable calibration procedures with argument-based prescribed decision-making rules for conformity assessment.

ACKNOWLEDGEMENT

This work was supported by the Ministry of Education and Science of North Macedonia under the Grant No. 15-6171/25.

REFERENCES

[1] M. Cundeva-Blajer, G. Dimitrovski, K. Demerdziev, V. Kafedziski, G. Josifovski, Calibration methods for high frequencies: Development and validation, Acta IMEKO, vol. 13 (2024) no. 3, pp. 1–7. DOI: 10.21014/actaimeko.v13i3.1764

[2] M. Cundeva-Blajer, Gj. Dimitrovski, M. Nakova, K. Demerdziev, Calibration of High Frequency Instruments-Evaluation of Uncertainty by Monte Carlo Approach, Proc. of the IMEKO TC8&TC11&TC24 Joint Int. Conf., Torino, Italy, 14–17 September 2025. DOI: 10.21014/tc11-2025.022

[3] S. Andonov, M. Cundeva-Blajer, TCal: Contribution to metrology for Industry 4.0, Jour. of Physics: Conf. Series, Vol. 1379 (2019), pp. 012021. DOI: 10.1088/1742-6596/1379/1/012021

[4] C. Cho, D. J. Lee, H. J. Goo, J. G. Lee, Frequency response of real-time digital oscilloscope with timeinterleaving architecture, 93rd ARFTG Microwave Measurement Conf. (ARFTG), Boston, MA, USA, 2019, pp. 1–4. DOI: 10.1109/ARFTG.2019.8739189

[5] D. Kim, J. G. Lee, D. J. Lee, C. Cho, Traceable calibration for a digital real-time oscilloscope with time interleaving architecture, Measurement Science and Technology, Vol. 29 (2018) Nr. 1, 015003. DOI: 10.1088/1361-6501/aa892c

[6] P. D. Hale, D. F. Williams, A. M. Dienstfrey, C. M. Wang, J. A. Jargon, (+ 4 more authors), Traceability of high-speed electrical waveforms at NIST, NPL, and PTB, Conf. on Precision Electromagnetic Measurements, Washington, DC, USA, 1-6 July 2012, pp. 522–523. DOI: 10.1109/CPEM.2012.6251033

[7] S. Rapuano, P. Daponte, L. de Vito, F. Picariello, I. Tudosa, N. Paulter, A Phase Measurement Method to Guarantee the Traceability of the Calibration Systems, Conf. on Precision Electromagnetic Measurements (CPEM 2020), Denver, CO, USA, 24–28 August 2020 (virtual), pp. 1–2. DOI: 10.1109/CPEM49742.2020.9191708

[8] BIPM KCDB, Calibration and Measurement Capabilities – CMCs and Key and supplementary comparisons, Online [Accessed 23 December 2025] https://www.bipm.org/kcdb

[9] EURAMET cg-7 Guidelines on the Calibration of Oscilloscopes, EURAMET Calibration Guide No. 7, Version 2.0 (09/20125). Online [Accessed 5 January 2026] https://www.euramet.org/publications-media-centre/calibration-guidelines

[10] Gj. Dimitrovski, M. Cundeva-Blajer, K. Demerdziev, Contribution to Improved Measurement and Calibration Capabilities in the Field of Measuring Instruments for High-Frequencies, Jour. of Electrical Eng. and IT Vol. 8 (2023) No. 2, pp. 101–107. Online [Accessed 5 January 2026] https://jeeit.feit.ukim.edu.mk/index.php/jeeit/article/view/378

[11] M. Cundeva-Blajer, Gj. Dimitrovski, V. Sapundziev, K. Demerdziev, V. Dimcev, Infrastructure Development for Extreme Electrical Metrology, Jour. of Electrical Eng. and IT 2022 Vol. 7 (2022) No. 2, pp. 101–109. Online [Accessed 5 January 2026] https://jeeit.feit.ukim.edu.mk/index.php/jeeit/article/view/348

[12] M. Cundeva-Blajer, Gj. Dimitrovski, K. Demerdziev Implementation and Validation of Calibration Methods in the Area of High Frequencies, Proc. of IMEKO TC8&TC11&TC24 Joint Int. Conf., Funchal-Madeira Islands, Portugal, 11–13 October 2023, 4 pp. DOI: 10.21014/tc11-2023.05

[13] Gj. Dimitrovski, M. Cundeva-Blajer, K. Demerdziev Contribution to improved measurement and calibration capabilities in the field of measuring instruments for high-frequencies, Int. Conf. MakoCigre 2023, Ohrid, North Macedonia, 17–19. September 2023.

[14] C. Cho, J. -G. Lee, T. -W. Kang and N. -W. Kang, Calibration of sample-time error in a sampling oscilloscope and uncertainty analysis, Conf. on Precision Electromagnetic Measurements (CPEM 2016), Ottawa, ON, Canada, 10-15 July 2016, pp. 1–2. DOI: 10.1109/CPEM.2016.7540669

[15] P. D. Hale, A. Dienstfrey, C-M. J. Wang, D. F. Williams, Traceable Waveform Calibration With a Covariance-Based Uncertainty Analysis, IEEE Transactions on Instrumentation and Measurement, vol. 58 (2009) no. 10, pp. 3554–3568. DOI: 10.1109/TIM.2009.2018012

[16] S. Pasakawee, V. Sittakul, Calibration and uncertainty evaluation of pulse generator for EMC testing using FFT technique, 13th Int. Conf. on Electrical Engineering/Electronics, Computer, Telecommunications and Information Technology (ECTI-CON), Chiang Mai, Thailand, 2016, pp. 1–5. DOI: 10.1109/ECTICon.2016.7561260

[17] D. F. Williams, T. S. Clement, K. A. Remley, P. D. Hale and F. Verbeyst, Systematic Error of the Nose-to-Nose Sampling-Oscilloscope Calibration, IEEE Transactions on Microwave Theory and Techniques, vol. 55 (2007) no. 9, pp. 1951–1957. DOI: 10.1109/TMTT.2007.904333

[18] Z. Jiangmiao, Z. Linxiao, G. Jian, M. Jingyuan, Z. Yueqian, Research on the uncertainty of calibrated bandwidth of broadband sampling oscilloscope, 13th IEEE Int. Conf. on Electronic Measurement & Instruments (ICEMI), Yangzhou, China, 2017, pp. 299–306. DOI: 10.1109/ICEMI.2017.8265958

[19] D. A. Humphreys, M. Hudlička, I. Fatadin, Calibration of Wideband Digital Real-Time Oscilloscopes, IEEE Transactions on Instrumentation and Measurement, vol. 64 (2015) no. 6, pp. 1716–1725. DOI: 10.1109/TIM.2015.2407471

[20] P. O. C. M. Neto, P. C. R. Brandão, J. C. M. Sanchez, L. C. de Almeida de Lima, C. E. C. Galhardo, Uncertainty Evaluation of the Electrical Transient Rise Time, IOP Publishing Ltd, Journal of Physics: Conference Series, Volume 1826, 10th Brazilian Congress on Metrology (Metrologia 2019), Florianopolis, SC, Brasil 2021, 24–27 November 2019, Ser. 1826 012103. DOI: 10.1088/1742-6596/1826/1/012103

[21] JCGM 100:2008 Evaluation of measurement data–Guide to the expression of uncertainty in measurement–GUM. Online [Accessed 5 January 2026] https://www.bipm.org/en/committees/jc/jcgm/publications

[22] JCGM 101:2008 Supplement 1 to the Guide to the expression of uncertainty in measurement- Propagation of distributions using a Monte Carlo method. Online [Accessed 5 January 2026] https://www.bipm.org/en/committees/jc/jcgm/publications

[23] M. G. Cox, A. B. Forbes, P. M. Harris, I. M. Smith, Measurement uncertainty evaluation associated with calibration functions, XIX IMEKO World Congress Fundamental and Applied Metrology, 2009. Online [Accessed 5 January 2026] https://www.imeko.org/publications/wc-2009/IMEKO-WC-2009-TC21-467.pdf

[24] B. F. Jamroz, D. F. Williams, J. D. Rezac, M. Frey, A. A. Koepke, Accurate Monte Carlo Uncertainty Analysis for Multiple Measurements of Microwave Systems, 2019 IEEE MTT-S Int. Microwave Symposium (IMS), Boston, MA, USA, 2–7 June 2019, pp. 1279–1282. DOI: 10.1109/MWSYM.2019.8701028

[25] M. Bieler, M. Spitzer, K. Pierz, U. Siegner, Improved Optoelectronic Technique for the Time-Domain Characterization of Sampling Oscilloscopes, IEEE Transactions on Instrumentation and Measurement, vol. 58 (2009) no. 4, pp. 1065–1071.

DOI: 10.1109/TIM.2008.2009916
[26] C. Cho, J. -G. Lee, J. -H. Kim and D. -C. Kim, Uncertainty analysis in EVM measurement using a Monte-Carlo simulation, 29th Conf. on Precision Electromagnetic Measurements (CPEM 2014), Rio de Janeiro, Brazil, 24-29 August 2014, pp. 700–701. DOI: 10.1109/CPEM.2014.6898578
[27] S. Eichstädt, A Link, P. Harris, C. Elster, Efficient implementation of a Monte Carlo method for uncertainty evaluation in dynamic measurements, BIPM & IOP Publishing Ltd Metrologia, Volume 49 (2012) Nr. 3, 401. DOI 10.1088/0026-1394/49/3/401
[28] S. S. Agili, A. W. Morales, J. Li, M. Resso, Finding the Probability Distribution Functions of S -Parameters and Their Monte Carlo Simulation, IEEE Transactions on Instrumentation and Measurement, vol. 61 (2012) no. 11, pp. 2993–3002. DOI: 10.1109/TIM.2012.2202165
[29] L. G. Lazaro, J. L. Quesada, A. Cerrudo, J. Ruiz, A. Alcantarilla, Generic implementation of Monte Carlo method for uncertainty evaluation. Application to calibration of RF power sensors, 2008 Conf. on Precision Electromagnetic Measurements Digest, Broomfield, CO, USA, 8-13 June 2008, pp. 254–255. DOI: 10.1109/CPEM.2008.4574749
[30] M. Cundeva-Blajer, M. Nakova, K. Demerdziev, Conformity Assessment of Impedance Parameters Meters by MonteCalc Uncertainty Toolkit, Proc. of the IMEKO TC8&TC11&TC24 Joint International Conference, Torino, Italy, 14–17 September 2025.
[31] M. Nakova, M. Cundeva-Blajer, Extension of the Calibration and Measurement Capabitilities of a Laboratory for Electrical Measurements and Application of the Monte Carlo Method for Evaluation of Measurement Unceratinty, 6th Int. Conf. Quality and Competence, Ohrid, R. N. Macedonia, 26–28 September 2024.
[32] M. Cundeva-Blajer, Data Fusion for Uncertainty Evaluation in Extreme Electrical Metrology, Proc. of Int. Cong. on Measurement, Quality and Data Science MQDS 2023, 5–7 June 2023, Bordeaux, France. Online [Accessed 5 January 2026] https://www.proceedings.com/content/070/070984webtoc.pdf
[33] EN ISO/IEC 17025:2017, General requirements for the competence of testing and calibration laboratories
[34] Transmille Ltd, Transmille 4000 Series Advanced Multiproduct Calibrator, Operation Manual, 2015. Online [Accessed 5 January 2026] https://www.transmille.com/product/4000-series/
[35] Rhode & Schwarz, RTO2000 Oscilloscope, Product Brochure Version 20.00, April 2021. Online [Accessed 5 January 2026] https://www.rohde-schwarz.com/cz/products/test-and-measurement/oscilloscopes/rs-rto2000-oscilloscope_63493-10790.html
[36] Rigol User's Guide DS1000E, DS1000D Series Digital Oscilloscopes, Publication No. UGA07118-1110 Dec. 2015. Online [Accessed 23 December 2025] https://www.rigolna.com/products/digital-oscilloscopes/1000/?srsltid=AfmBOoquwgffYYUTjFEO477cpcBigSi2M4JYmJtZF2fVlHr1-YsOJphZ
[37] GW Instek GDS-1000B Series Technical Specifications. Online [Accessed 23 December 2025] https://www.gwinstek.com/en-global/products/downloadSeriesDownNew/1738/130
[38] LabVIEW Programming Reference Manual, National Instruments Corporation, 2025. Online [Accessed 5 January 2026] https://www.ni.com/docs/en-US/bundle/labview-api-ref/page/intro.html?srsltid=AfmBOoqjrrZOkzzn5pu-I3Q8HZc6z9_flWNpt-XoTcWiPlTfjeV70_UB
[39] EN ISO/IEC 17025:2017 International Standardization Organization (ISO), General requirements for the competence of testing and calibration laboratories
[40] ILAC-G8:09/2019 Decision Rules and Statements of Conformity. Online [Accessed 5 January 2026] https://ilac.org/publications-and-resources/ilac-guidance-series/
[41] JCGM 106:2012, Evaluation of measurement data – The role of measurement uncertainty in conformity assessment.
[42] O. Velychko, S. Kursin, T. Gordiyenko, I. Pototskyi, Peculiarities of formation and checking of the accreditation scope of calibration laboratory, Measurement: Sensors, Vol. 38 (2025) Supplement, 101504, ISSN 2665-9174. DOI:10.1016/j.measen.2024.101504